Department of Precision and Microsystems Engineering

Improving power output of limited stroke automatic watch winding using a nonlinear transmission

Joep Meij

Report no : 2022.002
Coach : T. Blad, G. Dunning
Professor : J. Sprock
Specialisation : MSD
Type of report : master thesis
Date : 10 January 2022

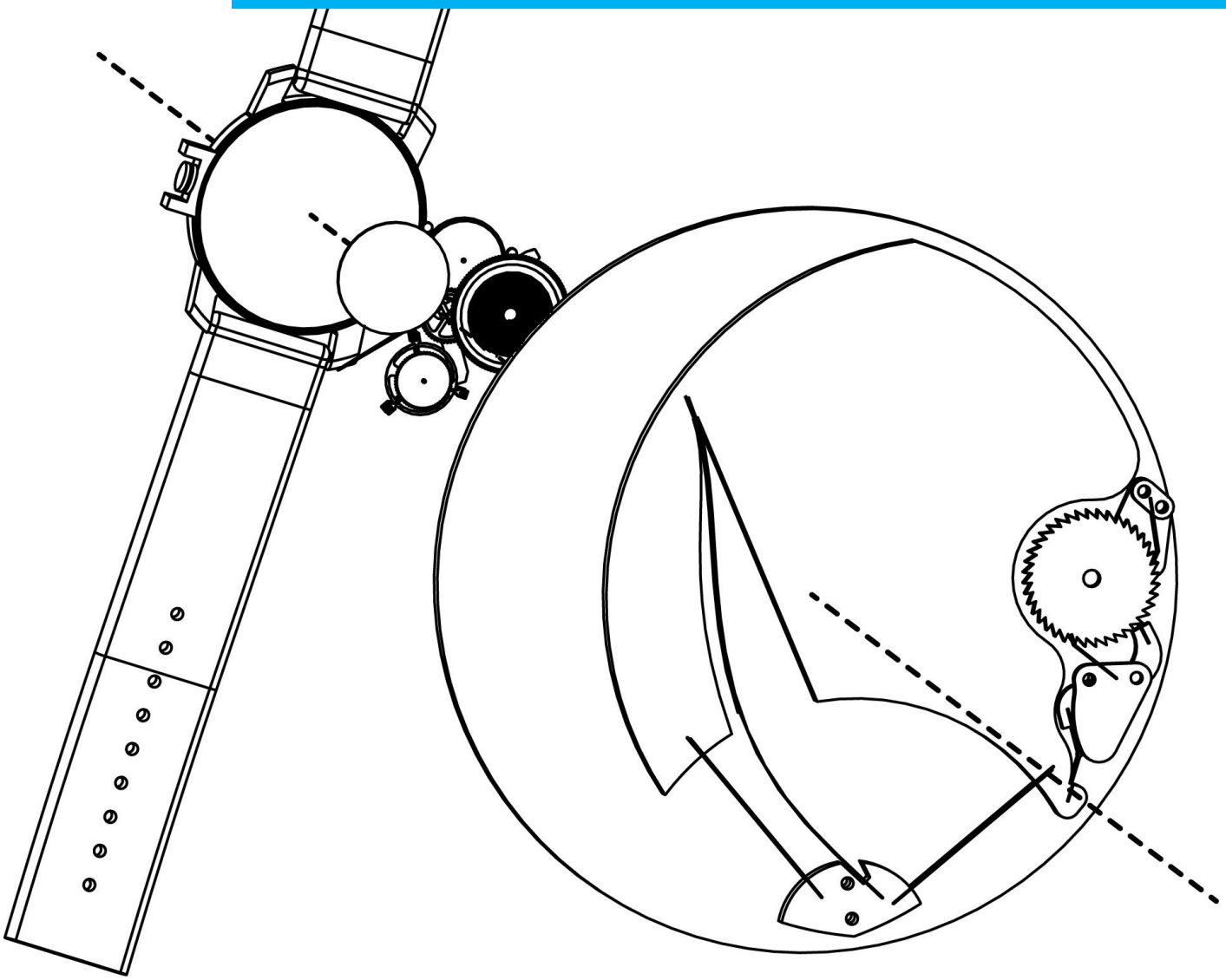

Contents

Abstract

Limited stroke automatic watch winding poses a challenge due to the proof mass range being smaller then the input displacements. Traditionally the proof mass is connected to the mainspring by a linear reduction transmission however this setup only functions effectively for specific accelerations. This paper proposes to use a nonlinear transmission between the proof mass and the mainspring improve the power output. This transmission will us a singularity to have a mechanical advantage of zero in the middle of its motion range, and increasing the further it moves. This improves the range in which the automatic winding device can operate especially the lower accelerations. A quasi static model of the system is made to estimate the efficiency of the mechanism for different accelerations which is verified by a demonstrator. These efficiencies combined with a human motion analysis suggest it could increase the energy generated to the mainspring by 52% compared to the linear transmission.

nomenclature

AW	Automatic winding
DAW	Direct automatic winding
PDAW	Period doubled automatic winding
Proof mass	Inertial mass used in inertial winding device
Mainspring	Energy storage of a mechanical watch
α	relative mainspring stiffness compared to acceleration
β	relative length of transmission rod compared to motion range

1 Introduction

1.1 Background

Automatic watch winding has been around for quite a while the first ones being made int he 18th century as shown on fig. 1.1 The man who pioneered the first mass produced automatic watch was John Hardwood. Just after the first world war John Harwood noticed that watches would often stop working due to dust and water coming in at the crown of the watch. He thought, what if one could wind a watch by other means and remove the crown to get rid of the entry point for dust and water. Harwood imagined a watch that was wound by the motion of the wearer. In 1923 he patented his invention of an automatic winding device to wind a watch which was based on an oscillating mass with a limited stroke. This type of winding was later known as 'pedometer' or 'bumper' type winding. Swiss manufacturers did not jump at the opportunity Harwood gave them. So automatic watches only slowly gained traction in the industry and Harwood's company went backrupt in the great depression. Meanwhile Rolex had improved the design by removing the limited stroke of the proof mass and creating the now well known 'Rotor' design. This type of automatic winding is the mechanism we still use today in our watches.

Figure 1.1: **automatic watch by Abraham Louis Breguet (Paris, ca. 1787)**

1.2 Rotor and limited stroke automatic winding

As shown before the limited stroke automatic winding lost out in favour of the rotor type design with unlimited stroke. This was due to the fact that the rotor design has two main advantages over the limited stroke type, it can use accelerations in two axis to store energy. And because of it's unlimited motion range it can store the potential energy imposed by the input accelerations temporarily as kinetic energy before storing it in the mainspring. This allows it to be more effective at extracting energy from different accelerations compared to limited stroke. As with limited stroke the mass would hit the endstop and lose energy.
However, limited stroke automatic winding could also have some advantages over rotary winding devices. Due to the proof mass not rotating the whole circle space is left on this plane for the other components of the movement like the ratchet or gear train. The rotational point of the proof mass does not need to be in the middle of the watch, allowing for more design freedom of this bearing. The systems can even be made compliant, to improve lifetime of the winding mechanism.
And with recent insight into energy harvesters based on oscillatory motion we now know pedometer

type devices can be optimized for the intended input motion. Maybe even outperforming rotary type winding devices.

(a) **(b)**

Figure 1.2: ***(a)* shows a modern limited stroke automatic watch *(b)* shows a modern rotor type automatic watch**

1.3 Compliant automatic winding

At flexous the goal is to combine compliant mechanisms with watchmaking to reduce the amount of parts in a watch improve precision and wear and tear. However for automatic winding this would mean that it will be impossible to make it a rotor type mechanism as this requires a full free spinning bearing. So here limited stroke automatic winding could make a comeback. A fully compliant automatic winding mechanism was already designed and tested. However performance was low, this mechanism worked only for specific activities because it did not handle varying input accelerations well and as stated before, it could not make use of multiple input axis. This had to be improved. And I chose to try to improve the efficiency of the mechanism for a wider acceleration spectrum. I suspected this could be done by creating a nonlinear transmission between the proof mass and the barrel spring of the watch. Normally this is a constant reduction in gearing. However what this nonlinear transmission should look like first had to be found out. In this thesis I will describe all the steps that where necessary to the results shown in the paper.

1.4 Outlline

To start, literature research was done on how energy harvesters improve upon the efficiency on human motion and what human motion looked like. From the literature search on energy harvesters the movement behaviour of the proof mass could be extracted for different accelerations. For the human wrist motion, I found a database of 10 different subjects doing different activities. Of all these activities, the accelerations and rotations where logged. Which proved later to be very useful. With this knowledge I proposed a new idea to use a nonlinear transmission in between the proof mass of the watch and the mainspring. The transmission would be a single linkage in its singularity position with linear bearings orthogonal to each other at both ends. This transmission would be compared to a normal reduction gear to find out if it yields any improvement. This analyses was done by analysing human motion data and modelling the winding device. And testing the hypothesis

on a demonstrator. First some initial exploring was done with the help of Simulink, this did show improvement in stored energy. To test this better a full numerical model was made combined with a physical demonstrator on a shaker. Verifying the mechanism this way proved to be difficult as the movement of the winding device became chaotic quite quickly and lots of values, like friction, stiffness of the mechanism and input motion where too difficult to acquire. However the demonstrator on the shaker and numerical model did show an increase of power output compared to a normal reduction gear. But proving how it worked and showing the underlying physics was impossible with the model because it depended on too many variables. Therefore a quasi-static model was made and verified on a physical demonstrator to prove the theory. With this quasi static model conclusions could be drawn which are written up in the paper. The numeric model and the shaker demonstrator setup have been moved to the appendix.

2 Literature review

This part will review the current solutions for harvesting energy from human wrist motion. It primarily looks at how non-linear characteristics of the harvester will change the behaviour of these systems thus changing the efficiency. In the field of energy harvesting much work has been done on harmonically tuned or broadband systems with small vibrations. So a research gap is left for high amplitude non-harmonic energy harvesters which play a significant role in real world scenario's, especially body motion. First human wrist motion is reviewed then how a linear energy harvesting converts this to stored power then nonlinear systems will be reviewed to see how they behave on the human wrist. Starting with nonlinear stiffness and then nonlinear energy conversion. The goal will be to see if winding devices for horology can be improved by changing their characteristics.

2.1 Literature revieuw introduction

With the increasing efficiency of electronic devices like radio transmitters, microprocessors and sensors. The opportunity emerges to power these electronics not by wire or battery but by environmental power sources like heat, light, motion or magnetic fields. This has the advantage of allowing portability without the need of charging. Even with non-portable systems it could yield a benefit in eliminating wiring to power a device or sensor and getting power to places where it previously could not get. [1]
Using these energy harvesting devices on the human body to charge small electronics and sensors could prove useful for medical devices or small consumer electronics. A study from J. yun et al. In 2008[2] showed the available power for an on body harvesters could just about power a gps chip. This showed promise but improving the power yield is essential to make it more usable for more power hungry components like screens or processors.
To increase power yields of energy harvesters we often look for periodic motion of a system and design a specific energy harvester for that type of movement by changing its stiffness or damping. For static machines with continuously rotating components this is relatively easy, as these components often create harmonic vibrations with small amplitudes. These vibrations allow for Linear Resonant(LR) harvesters to be viable, which reach estimated efficiencies of around 10% [3].
Human body motion however is of a different kind. The amplitudes and periodicity change with the placement of the harvester and with the activity the person is performing[4]. This has been shown to be a difficult problem to solve, if a harvester works well for one activity it might not work effectively for another. Even the size of the harvester matters for what architecture to choose from [1]. Research has always simplified one or the other, if a nonlinear architecture is explored, the motion will be simplified to a periodic excitation like walking or shaking[5, 6, 7, 8]. If non periodic human motion is taken into account the energy harvester is simplified to a linear architecture[2]. This done to keep the complexity down, but also because there is no standard measurement of human motion to compare effectiveness of a harvester.
Reverting to a periodic movement like walking is the simplest option. But Tudor-locke et. al.[9] estimated that only 31% of american adults would go over 7500 steps per day, which correlates to about 90 minutes per day. Testing an and designing an energy harvester on just the walking gate means energy output is based on a periodic motion which is only performed for 6% of the day. Improvement could potentially be made if harvesters could wield a wider set of human activities with periodic and nonperiodic motion.
This paper will create an overview of current inertial energy harvesting designs and evaluate if they could prove useful for human wrist motion. The first section evaluates human wrist motion. Then a section on a basic velocity dampened resonant generator(VDRG) and their working principles, after that we show how current nonlinear energy harvesters differ in nonlinear stiffness and nonlinear damping, and how this influences performance.

2.2 Human wrist motion

Human wrist motion varies wildly with different activities. This makes energy harvesting from this type of motion difficult and interdisciplinary. Thus almost all technical papers about an energy harvesters for human motion are simplified to walking. This section will further explore what human motion entails to gain insight in how it should determine energy harvester design.
Research into human behaviour have been quite extensive and give good insight into how time is spend. fig.2.1 from [10] shows how much time an adult spends doing an activity during the day. This was done using wearable accelerometer data and a camera to check the activity.

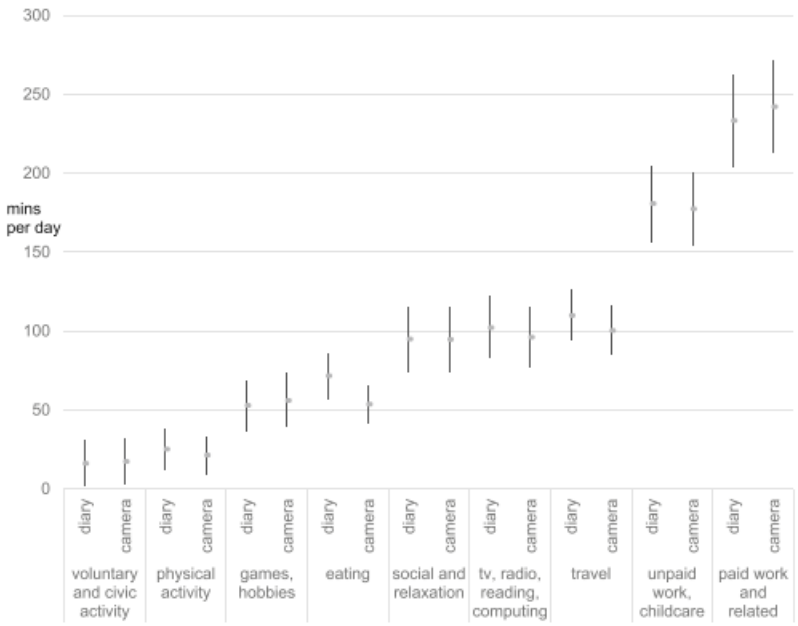

Figure 2.1: **from [10] time spend per activity per day**

This study had 148 participants and would give a reasonable estimation of time use. Here sleep was not counted as an activity and it can clearly be seen most of the time is spend doing work, unpayed or payed. Then come travel, watching tv, and social activities. And at the lower end of the time use are physical activities. When looking at these activities from an energy harvesting point of view they can be classified by intensity which is done in [11]. in fig2.2

Table 2. *Activity types, categories, and intensities performed in the protocols*

Activity Type	Activity Category	Activity Intensity	Compendium Code
	Michigan State University data		
Lying down	Sedentary	Sedentary	07010
Reading quietly	Sedentary	Sedentary	07070
Using a computer	Sedentary	Sedentary	07021
Standing	Household	Light	07041
Sweeping	Household	Light	05011
Folding laundry	Household	Light	05090
Walking slowly (overground)	Ambulatory/exercise	Light	17152
Walking briskly (overground)	Ambulatory/exercise	Moderate	17190
Jogging (overground)	Ambulatory/exercise	Vigorous	12020
Cycling (stationary, 50–100 W)	Ambulatory/exercise	Moderate	02017
Stair use	Ambulatory/exercise	Vigorous	17134
Squats (body weight)	Ambulatory/exercise	Moderate	02052
Biceps curls (1.4-kg dumbbell per hand)	Ambulatory/exercise	Light	02024
	Ball State University data		
Lying down	Sedentary	Sedentary	07010
Using a computer	Sedentary	Sedentary	07021
Watching television	Sedentary	Sedentary	07020
Writing	Sedentary	Sedentary	07050
Playing cards	Sedentary	Sedentary	07021
Reading quietly	Sedentary	Sedentary	07070
Standing	Household	Light	07041
Dusting	Household	Light	05032
Making bed	Household	Light	05040
Folding laundry	Household	Light	05090
Sweeping	Household	Light	05011
Vacuuming	Household	Light	05040
Gardening: scooping dirt with hand shovel	Household	Light	08135
Picking up items (<1 kg) off floor	Household	Moderate	05030
Walking slowly (overground)	Ambulatory/exercise	Light	17152
Walking briskly (overground)	Ambulatory/exercise	Moderate	17190
Self-paced walking (treadmill)	Ambulatory/exercise	Moderate	17190
Cycling (stationary, 75–150 W)	Ambulatory/exercise	Moderate	02017
Stair climbing/descending	Ambulatory/exercise	Vigorous	17134
Overground jogging	Ambulatory/exercise	Vigorous	12020
Treadmill jogging	Ambulatory/exercise	Vigorous	12020

Figure 2.2: **from [11] intensity of daily activities**

When 2.1 and fig.2.2 are combined it can be seen most of the time is spend doing light of even sedentary tasks. This intensity shows the potential of energy to be harvested with different activities. Bus also shows that optimizing for just one moderate or vigorous task would mean large storage capacity is nessecary to bridge the gaps of sedentary and light activity. How these activities correlate to accelerations and frequencies of the wrist is shown in an extensive study by reiss et al. [4]. Where 9 participants where asked to do physical activities. Which where measured by accelerometers worn on the hip, the wrist and the ankle. From this high quality acceleration data can be extracted for 24 different activities. And the difference in activities can be clearly seen. Fig.2.3

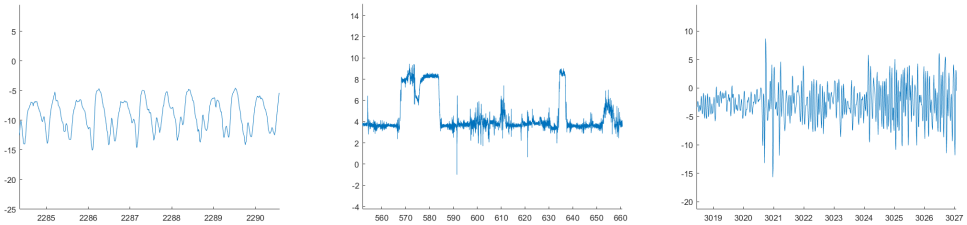

(a) **(b)** **(c)**

Figure 2.3: **[4]acceleration data from a single axis in line with the forearm from different activities with g force on the vertical and time on the horizontal axis *(a)* walking. Fig. *(b)* computer work *(c)* cycling**

Here the difference in periodicity and acceleration can clearly be seen walking shows a clear periodic signal whilst computer work is clearly non-periodic and does not have a lot of motion. Cycling gives a wide band of frequencies and amplitudes. For most activities the amplitudes would be within a range of about $\pm 2.5G$. So for an energy harvester to be able to capture energy from human activities it must be able to harvest energy from periodic as well as non periodic excitation. On a wide spectrum of excitation amplitudes at low frequencies. So the human wrist motion consists of different activities with periodic and non-periodic motion. Where the periodic motions have very low frequencies mostly within the range of $0 - 15Hz$ and accelerations within $/pm2.5G$. almost all of the motion has high displacement compared to the internal displacement of a wrist worn harvester.

2.3 Inertial energy harvester

2.3.1 Linear energy harvester and harmonic motion

To convert motion to usable energy, generators are used. Generators take many different forms, alternators or dynamo's on a car or bike to bigger ones in power stations. What separates energy harvesters from generators is that they use energy which is otherwise kept unused. Motion driven energy harvesters can be distinguished in two types. Those that use direct force to generate energy an those that use the inertia of a mass to generate that force. This paper focuses on inertial harvesters as they don't require a force to be exerted on something which makes them better suited for wrist worn applications. The most basic inertial energy harvesters comprise of 3 parts, a mass, a spring and a damper which generates the energy. To tune and predict these systems they can be modeled as a mass spring damper system in a box shown in fig. 2.4

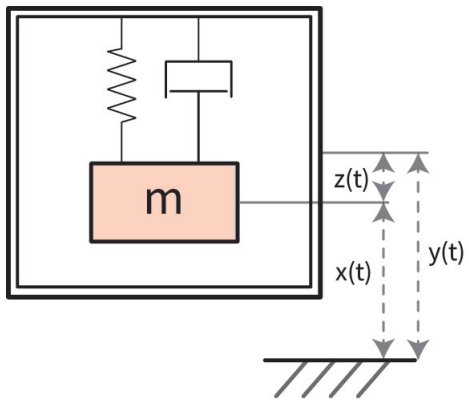

Figure 2.4: **mass spring damper system**

Displacement $y(t)$ is the input motion of the harvester, if the harvester is displaced the inertia of the mass will bring about a relative displacement $z(t)$. This will do work on on the damper which converts this energy to a usable form.
With velocity dampened resonant generators(VDRG) the damping force is proportional to the relative speed of the mass $\dot{z}(t)$ with constant D. To maximize the energy output of such device it must be excited by its resonant frequency, this will generate the highest relative speed between the frame and the mass thus optimizing power output. In this case stiffness and damping should be optimized for maximal allowed displacement at resonance. Which was shown in [12].
This paper also showed that with a sinusoidal input motion it had a power output per cycle of.

$$P = \frac{\zeta \omega_c^3 Y_0^2 \omega^3 m}{[1 - \omega_c^2]^2 + [2\zeta\omega_c]^2} \tag{1}$$

where ω_c is the fraction of the input frequency to the eigenfrequency. $\omega_c = \omega/\omega_n$ with the eigenfrequency being $\omega_n = \sqrt{k/m}$ when the optimum damping was chosen, maximum power would be generated at $\omega_c = 1$ is:

$$P_{res}\frac{1}{2}Y_0^2\omega m\frac{Z_l}{Y_0} \tag{2}$$

here we can see what limits the power at resonance when the system is not displacement limited. Yun et al. [2] investigated if this could be used for harvesting energy from human motion by tuning these systems to the dominant frequency of the wrist. With a proof mass displacement and mass of 42mm and 2g respectively. This gave an average power output of $155 \pm 106\mu W$. We can see this has huge variation, which can be explained by the behaviour of this system if used for non-resonant sources. yang et al. [3] investigated this. When an VDRG is excited by harmonic motion it will create a system response. Which was shown in [3] shown in fig.2.5

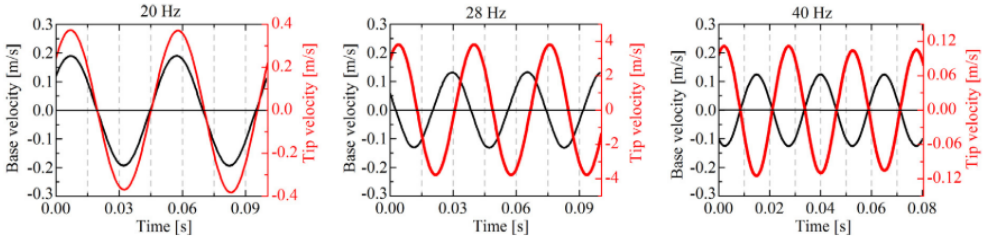

Figure 2.5: **plot from.[3] velocity response of mass(red) x(t) and frame(black) y(t) of a system with 28Hz resonance.**

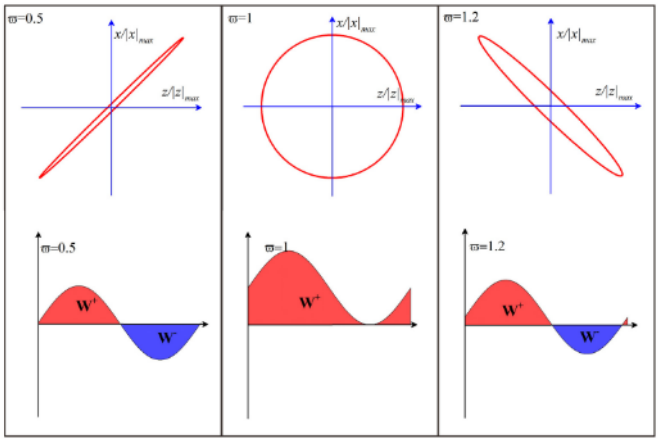

Figure 2.6: **schematic from.[3] work put in to an osscillator**

The response shows three frequency regimes such a harvester can operate in: lower then resonance, at resonance, and higher then resonance. The schematic 2.6 shows what happens to the energy flow of an VDRG system when excited in these regimes. The total work done on the system is $W_{tot} = W^+ - W^-$. When the system is at resonance, all of the energy will be converted to internal kinetic energy of the mass. As the energy output is relative to the speed of the proof mass, this will maximize power output. In the lower and higher then resonance regime, the spring effectively gives back the energy to the source. This will have a detrimental effect on the energy harvesting capabilities in these regimes.

As human motion is only partially periodic, and almost never harmonic this could explain the variation. This was also found by Yun [2] as the power varied greatly per activity. Due to different activities have different available powers and frequencies. The study however was purely theoretical and harvesters designed with a resonant frequency designed for human motion between 0 to $10Hz$ on the scale described would be rather difficult to realize due to scaling laws increasing the frequency. This makes the VDRG not very suitable for human motion, therefore we can look further then the linear case.

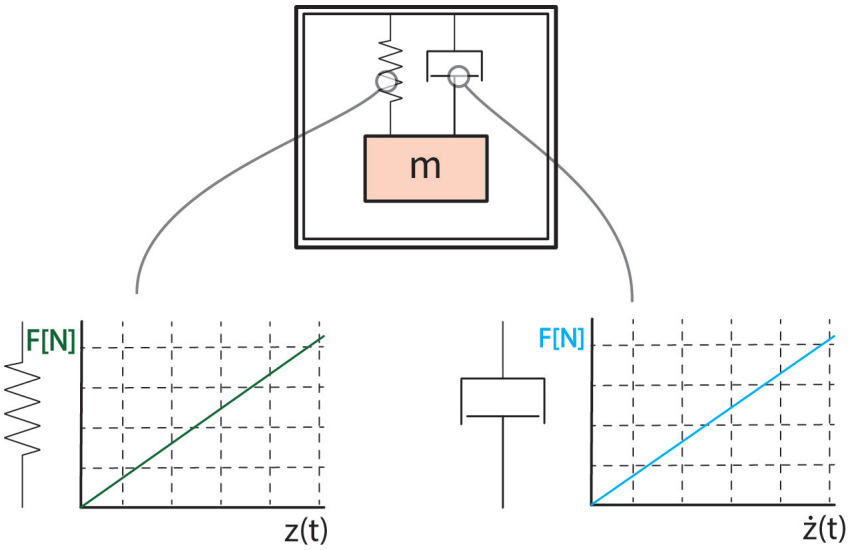

Figure 2.7: **mass spring damper system**

Fig. 2.7 resembles a VDRG. When it is limited by size and weight which is the case on a wrist worn harvester. The spring and damper curves still allow for some design freedom. By using nonlinear spring or damping curves the behaviour, an thus energy output, of the system can change drastically. This is what the next sections will be about.

2.4 Nonlinear stiffness

Nonlinearities in energy harvesters where introduced to create a more broadband energy harvester. As stiffness can be altered infinite amount of ways, there are some which have been researched. In fig. 2.8 the different nonlinearities described later are shown. All the systems described in this section and shown are the open terminal voltage.

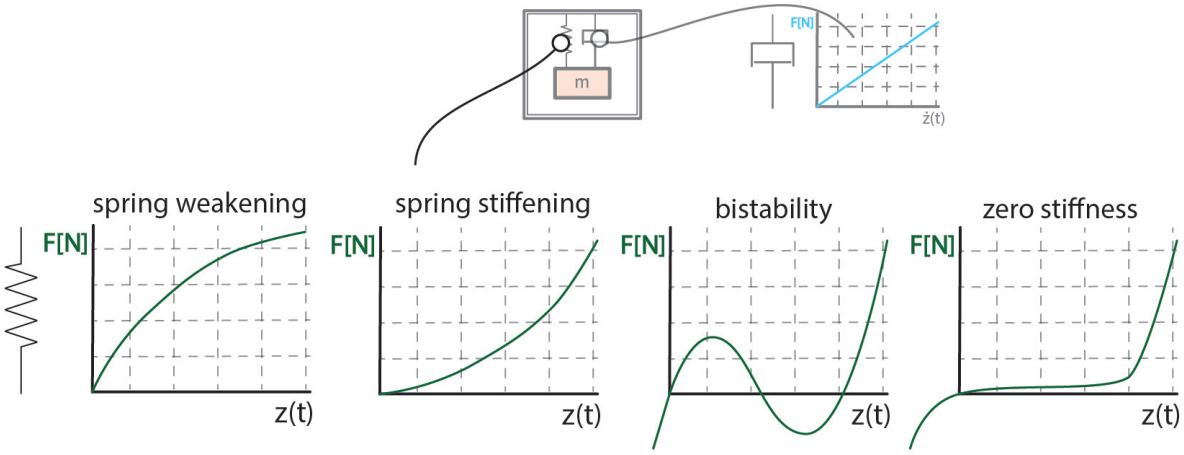

Figure 2.8: **nonlineair stiffness harvesters**

2.4.1 Spring stiffening and weakening

spring stiffening or spring weakening are the simplest type of nonlinear stiffness. These systems have been researched other fields under the category of duffing oscillators. These duffing oscillators widen the resonant frequency band but only under specific circumstances. Also they create unstable frequency responses where the resonance can occur and disappear suddenly.

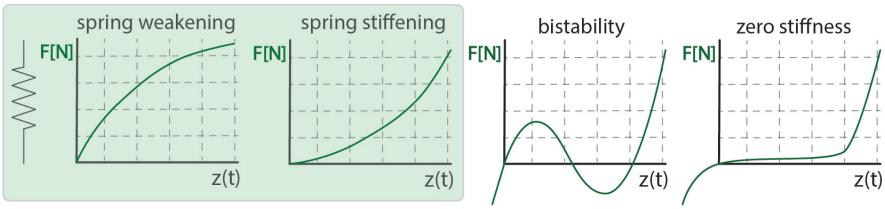

Figure 2.9: **spring weakening and stiffening**

These systems are also described by yang in [3] with a frequency sweep where the instability can be seen. If approached from below a stiffening system increases its amplitude untill it reaches a point where it instantly drops to almost zero. When approached from a higher frequency the inverse happens but for a smaller bandwith. A softening system has the same response but inverted as shown in fig. 2.10

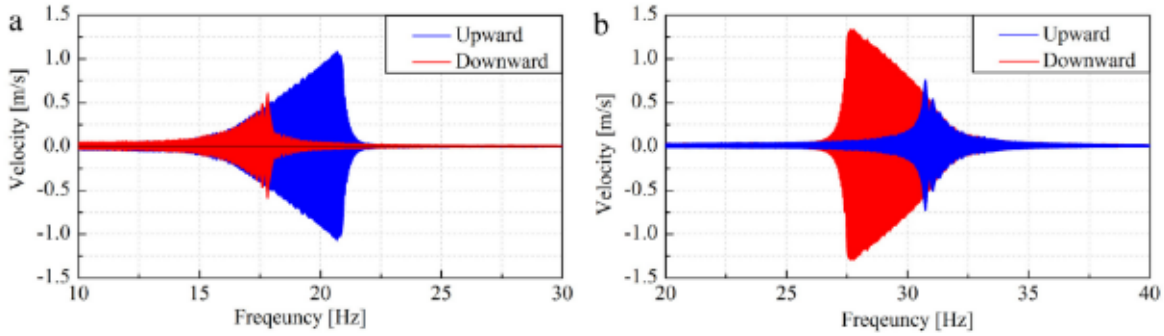

Figure 2.10: **plot from [3] frequency sweep hardening and softening duffing oscillator a)hardening b)softening**

Daqaq et al. showed in [13] evaluated such a harvester with the use of an axially loaded beam. Which when excited showed behaviour similar to a spring stiffening energy harvester. He showed these systems could be tuned for different frequencies by changing the axial load on the beam.
The main reason these systems will not work for Human motion is that they still require a driving frequency to make use of their wider frequency band. If not approached right they wont be able to harvest energy from certain frequencies.

2.4.2 Bistability

Bistable energy harvesters have shown promise in harvesting low-frequency high amplitude motion. Due to their tunable negative stiffness low frequencies can be reached at small scales. However Bistable havesters have three operating regimes interwell intrawell and chaotic. These regimes, like the regimes of the VDRG's depend on frequency and amplitude at which they need to be tuned towards[8]. This unfortunately means bistable harvesters are not the one-size-fits-all harvester which are required for human motion.

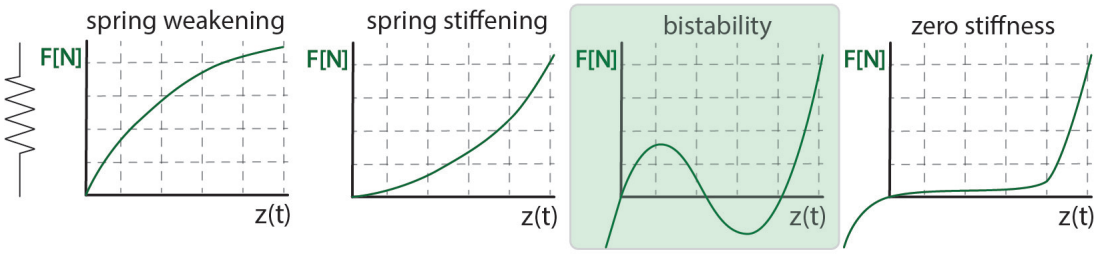

Figure 2.11: **bistable energy harvesting**

Bistable mechanisms are not new and are in use in products today Like light switches, grippers or peppermint boxes. These all possess the same behaviour in the stiffness curve shown in fig.2.12. When a load is exerted the stiffness will slowly decrease until it becomes negative. At this point the mechanism will will experience so called 'snap through' behaviour and it will snap to its second stable position.

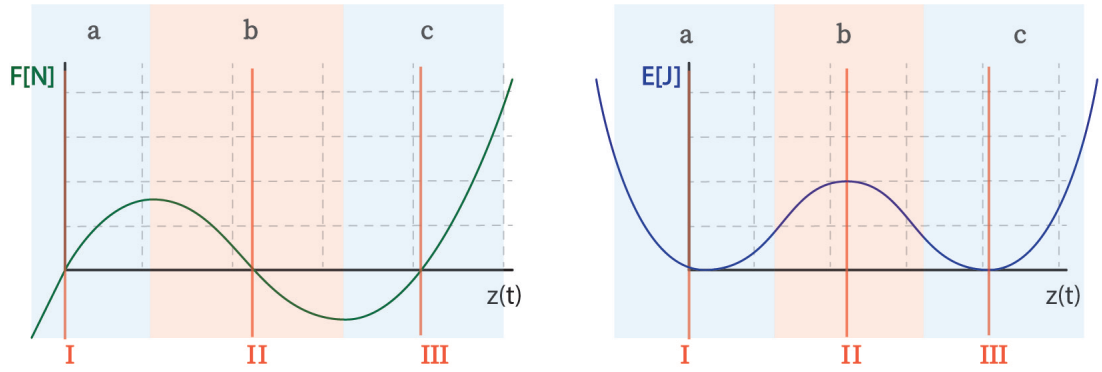

Figure 2.12: **bistable stiffness and energy curve with equilibrium's**

This can be explained further when looked at the stiffness curve. A bistable stiffness curve consists of three regions denoted as a, b and c and tree equilibrium positions denoted as I, II and III in fig. 2.12. in region a and c the mechanism has a positive stiffness and in region b it has a negative stiffness. This creates three equilibrium positions, the positions where $\delta E/\delta z = 0$ or where the force is zero. Points I and III are stable equilibrium's and II is an unstable equilibrium. This is because the second derivative at point II gives $\delta E^2/\delta^2 z < 0$. This point can be seen as the top of the energy barrier between I and III.
This energy barrier has been shown to be an important factor when used in energy harvesting[14]. The excitation amplitude should be high enough to force the mass over this energy barrier. If the excitation amplitude is too low the proof mass will stay in one of the energy wells and behave like linear energy harvester with less displacement. As power output is depended on the displacement, shown on the section on VDRG's, this will decrease output power. This effect of the energy barrier can easily be seen in 2.13 where the output voltage of the system at $4m/s^2$ is significantly lower then at $5.85m/s^2$

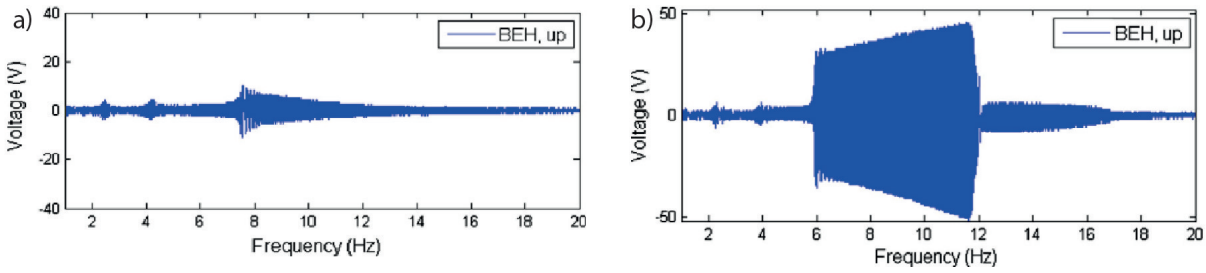

Figure 2.13: **from: [14] bistable energy harvester frequency sweep at different amplitudes a)**$4m/s^2$ **b)**$5.85m/s^2$

Green et al.[8] investigated how bistable harvesters performed when used in human walking motion. Here they performed worse then its linear monostable counterpart. For bridge motion, with a more spread out frequency spectrum it would perform similar to the linear counterpart. Green showed that if the goal is maximal power output bistable harvesters will most likely not make sense. But if size an low frequency is necessary bistable harvesters would make sense. With the bistable mechanism the stiffness can be tuned more independently of the mechanism size compared to it's linear counterparts. This makes them easier to tune for low frequencies like human motion as linear harvesters would require weak springs and high masses. This can prove especially difficult when going to micro scale.

Cao [15] et al. however proved the opposite by an experiment with a bistable harvester attached to the leg of a subject. Here the bistable harvester outperformed the monostable harvester at any walking speed.

2.4.3 Tristable and zero stiffness

Multistable mechanisms are created when multiple stable equilibrium's exist in the stiffness curve. If a mechanism is created with infinite stable equilirium's quasi zero stiffness can be created. For energy harvesters this means the harvester will not have an Eigenfrequency and will be able to operate in a low frequency band. Also because the lack of an energy barrier like bistable systems these systems will be less influenced by a change in amplitude. However these systems still need to be tuned to an amplitude, which can be done by changing damping or range of motion. This means zero stiffness harvesters have a lot of potential in low frequency and non periodic input motion. First we will look at the tristable energy harvester from [14]. Then further to zero stiffness mechanisms.

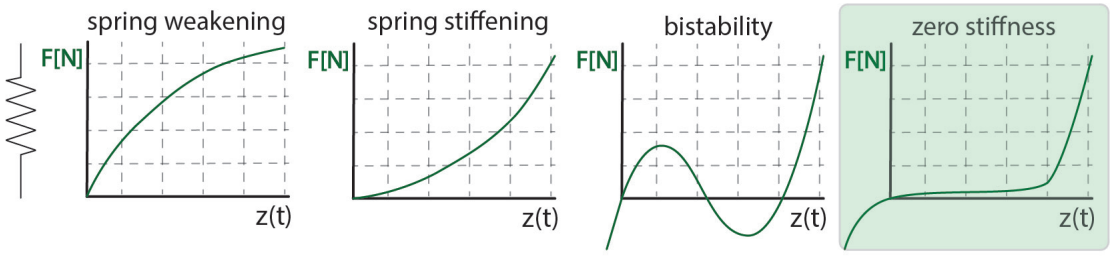

Figure 2.14: **zero stiffness**

Zhou et al.[14] showed with the use of magnets a tristable mechanism for energy harvesting could be realized. It was compared to a very similar bistable mechanism. In both amplitude and frequency range the tristable mechanism outperformed the bistable meachism. In the frequency sweep of these system it is clearly visible it has a wider usable frequency spectrum compared to its bistable counterpart.

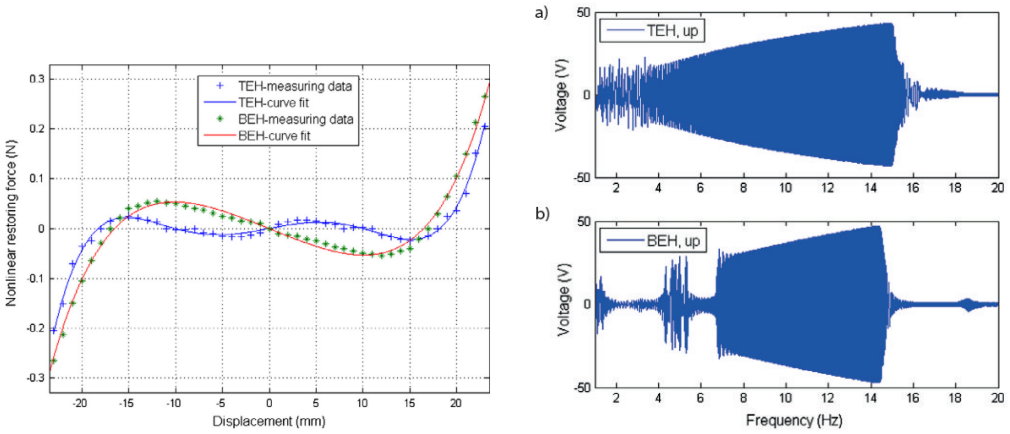

(a) **(b)**

Figure 2.15: **from [14]comparison tristable to bistable mechanism with frequency sweep.** ***(a)*** **shows the stiffness curve of both the bi an tristable harvester. Fig.** ***(b)*** **a) shows the frequency sweep of the tristable havester and b) of the bistable one.**

in fig 2.15 is is clearly seen the tristable harvester outperforms the bistable harvester in the lower frequencies. furthermore Zhou also showed the difference in input amplitude. Where the behaviour described in 2.13 did not show up for the tristable harvesters. This does not mean tristable harvesters will not experience this behaviour, tristable energy harvesters do have an energy well. But the energy barrier is most likely lower. This means that for lower amplitude input motion the tristable harvester will also give large deflection. In fig.2.15a the stiffness of the tristable mechanism can be seen, if the amount of stable points are increased to infinity a zero stiffness system is created. Zero stiffness mechanisms have similar properties to the tristable mechanism's in their low frequency potential.
The similarities can be clearly seen in [16] fig. 2.16 where a quasi zero stiffness device was tested it showed similar responses to the tristable system shown in fig. 2.15. The system has two operating regions which are divided by the jump down frequency. They operate well between zero Hz and their jump down frequency, and after that damping will take over and hold the proof mass in place. The frequency range, like spring stiffening and weakening, still depends on how the system is approached. From a higher frequency or from zero frequency.

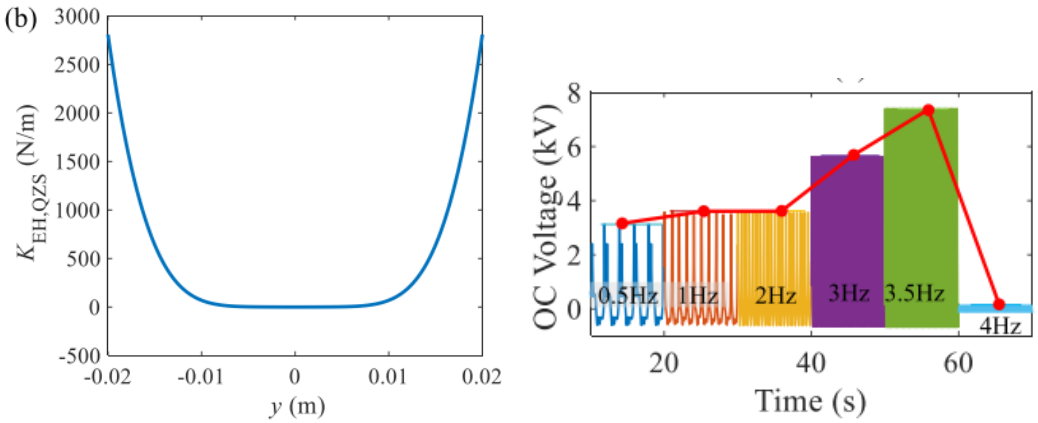

(a) **(b)**

Figure 2.16: **from [16]quazi zero stiffness energy harvester with *(a)* shows the stiffness curve of the quazi zero stiffness device Fig. *(b)* shows voltage output with changing frequency over time**

For human body motion With a combination of non periodic and low frequency motion. A zero stiffness harvester could prove to be very useful as it can perform well in both. Also due to the very low frequency band and non existent energy wells. A zero stiffness harvesters would perform best in the combination of human activities.

2.5 Nonlinear energy conversion

The damping of the system, or the energy conversion mechanism from motion to energy influences the internal motion of the mass. This influences, like stiffness, the behaviour of the harvester. In this section will look at different damping solutions which have been explored. It will not look at how the energy is converted electrically or mechanically. But rather how damping influences the harvesting potential. For human motion Nonlinear and active damping have been explored to be able to cope with the changing frequencies and amplitudes. Active damping systems have been used with varying success, for small harvesters the challenge is to let the active system consume less energy then the harvester is producing.
This section divides damping in three sections, viscous damping, coulomb force damping, and an experimental type coulomb force parametric generator. Again as with the section on stiffness we'll look at some research that have been done on the subject and if it can be used for the human wrist motion.

2.5.1 Viscous damping

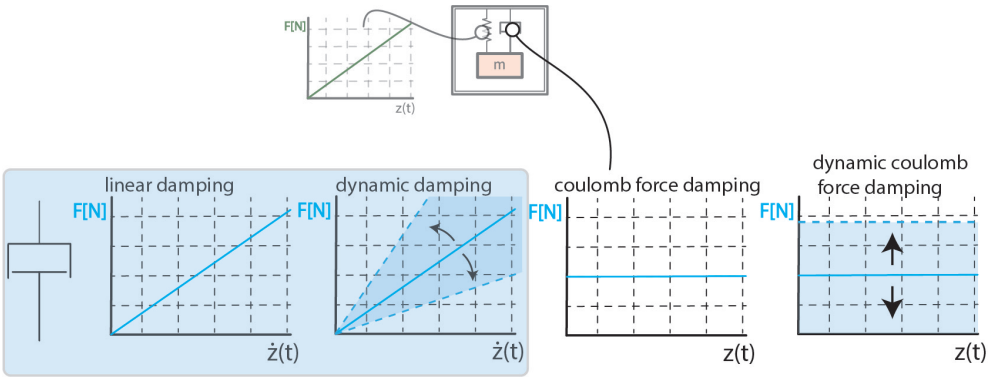

Figure 2.17: **viscous damping**

Velocity based damping is one of the most used damping systems in energy harvesters. This is mostly due to the energy conversion mechanism being a magnet and coil moving relative to each other. As the energy potential of velocity based conversion mechanisms depend on speed, this type of damping will favour high frequencies. Which for VDRG's is at their resonant peak's. This can be clearly seen in a paper from [17]. Here a theoretical model of an energy harvester with different dampers is optimized to find the output powers of such devices. It was shown that when a resonant energy harvester extracts too much energy, it is dampened too much, it wont be able to increase its amplitude to make full use of it's resonance peak. Thus for resonant devices damping is chosen as low as the displacement of the proof mass allows. Maximizing the output power. This example shows how important damping can be for an energy harvester.
However when the damping is optimized for it's resonance peak it will have less perfomance when it is not at resonance. If active damping can be used, where damping is actively varied with changing input frequencies the plot in fig.2.18

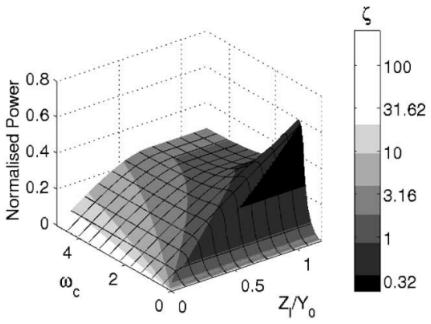

Figure 2.18: **from [17] VDRG with normalized power**

The plot shows an actively dampened resonant harvester. Here the decrease in power is still clearly seen when not at resonance. Also when used in human body motion this will only work for periodic motion as the damping will have to be be tuned towards excitation amplitude and frequency to get the most power out of the harvester. So velocity dampened resonant generators could work well for human body motion if actively tuned towards a periodic excitation. Also as seen in fig. 2.18

the normalized power rapidly drops when the excitation frequency is lower then the eigenfrequency of the harvester. Meaning the eigenfrequencies of the harvesters should be equal or lower then the lowest frequency of human body motion, Like walking.

2.5.2 Coulomb force damping

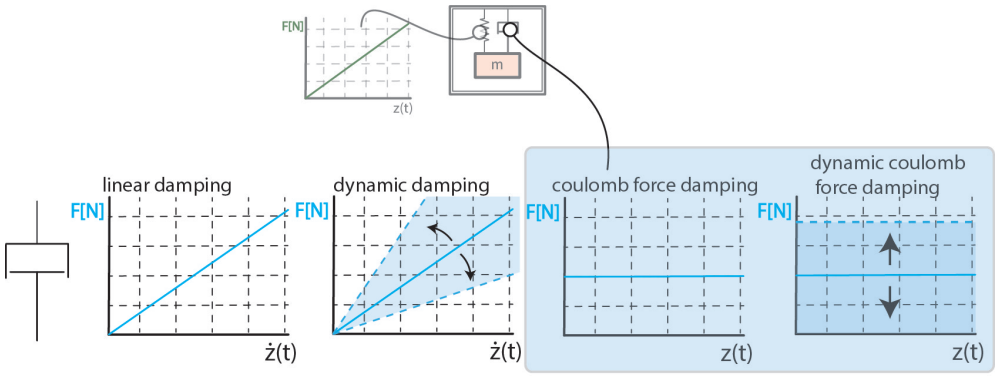

Figure 2.19: **viscous damping**

Displacement based damping means the force extracting energy from the system is constant and not dependent on the velocity of position of the harvester. This was shown in [17] as an electrostatic energy converter the coulomb dampened resonant generator(CDRG). It showed a similar normalized power output graph to the VDRG with respect to the shape, with a few distinct differences. It would not provida any power if the displacement limit was too small. At that point the damping force to stay within displacement dimensions would be too large to move the mass. Also the power would taper off more then the VDRG at higher frequencies.

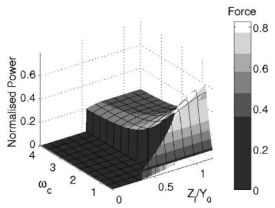

Figure 2.20: **from [17] CDRG normalized power**

For harvesting from human body motion it would not improve over the VDRG but power output over the whole range of excitation frequencies and amplitudes would stay relatively similar. The behaviour of the harvester however would change drastically shown in [18] where the harvesters from [17] where tested on a harmonic excitation. Here the difference in behaviour can be clearly seen in both systems in fig. 2.21 . Where the CDRG experiences stick slip at the points where acceleration is not high enough whereas the VDRG does not have this behaviour. Both systems utilize the same travel range of the proof mass and hence have similar power output performance.

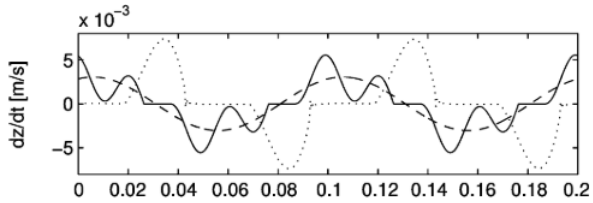

Figure 2.21: **from [18] VDRG dashed line. and CDRG solid line**

So performance wise the CDRG does not inprove power output, it rather decreases a bit. And it does not provide any power if the excitation amplitude gets below a certain threshold. But a different type of damping allows for more conversion mechanisms to be used.

2.5.3 CFPG

Mitcheson et al. [17] proposed the CFPG which is a more experimental type of energy conversion. Where the proof mass would be released ad maximum acceleration. This CFPG was researched further in [19] and [18] where it proved to work well for high displacement non periodic excitation. This makes sense as when the power output is limited by the internal motion of the proof mass, the energy produced can be increased by increasing the force acting on the mass during the internal motion.
This type of harvester does not have an eigenfrequency but will move the maximal distance at highest accleration to extract the maximum energy from the motion within the limitations of the harvester. This type of harvester has been theoretically conceived and experimentally tested in [12]. It showed it could work for a very wide range of motion. Especially low frequencies and high amplitudes which makes them very useful for human motion. It does however need to be actively tuned during excitation to ensure the proof mass has zero relative velocity when reaching the end of its stroke. A second experimental type was shown in [19] where a ratchet mechanism was proposed to create a similar motion pattern for the inertial mass as the the CFPG proposed in [12]. Where the inertial mass would be at maximum displacement $\pm z_{max}$ and would start moving at maximum acceleration. It was shown that this type of harvester would theoretically be better then both a linear and bistable mechanism for a wide range of motion.

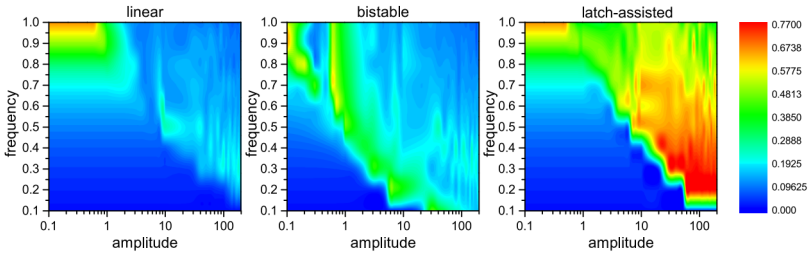

Figure 2.22: **from [19] the latch assisted CFPG compared to linear and bistable system on a varying range of frequencies and amplitudes**

This makes this system one of the most promising harvesting solutions for human body motion. As it is unbounded by frequency and acceleration and does not need any resonant motion to operate. The study showed that also for walking the latch assisted mechanism(CFPG) would outperform the linear and bistable system, the study did not take into account any inefficiencies of converting power. It just focussed on the theoretial possible power. When these inefficiencies are taken into account which was done in a study from Büren et al. [18] where it showed linear harvesters would

outperform a CFPG when used in in walking motion. So if a more effective way of converting power and holding the proof mass is found a CFPG will be most effective for human motion.

2.6 Conclusion

When designing energy harvesters for human motion one must take into account the wildly varying acceleration profiles at different activities, the high displacements compared to the size of the harvester and that human motion consists of periodic and non periodic activities.
If a harvester is designed for all of these specifications it should work well for accelerations within the range of $/pm2.5G$ with frequencies ranging from 0 to about $15Hz$. For this type of all-round harvester we looked into harvesters with nonlinear stiffness and nonlinear energy conversion. When looking at the stiffness a device with very low or zero stiffness would most likely perform best. Such devices will be able to work within the very low frequency ranges required and do not need a specific acceleration, like bistable systems do, to operate. Also zero stiffness systems will not require resonance to function well.
Nonlinear energy conversion can be divided into two categories viscous damping and Coulomb force damping. For energy harvesters with changing excitation it is best to dynamically change the damping values accordingly to allow for maximum displacement of the harvester. For excitation that consists of a combination of periodic and non periodic motion with high displacements, CFPG type of damping can be used best. This will theoretically allow for maximum power output of the system, thus making them viable for human motion. This is however very dependent on the conversion mechanism of kinetic energy to another form usable energy. As different conversion mechanisms will change efficiencies at different scales.

Article

3 Improving power output of limited stroke automatic watch winding using a nonlinear transmission.

J. Meij[1], T. W. A. Blad [1], G. Dunning [2], J. Spronck [1]

[1] Department of Precision and Microsystems Engineering, Delft University of Technology, 2628 CD Delft, The Netherlands.
[2] Flexous, Molengraafsingel 12, 2629 JD Delft ,Netherlands

Correspondence: t.w.a.blad@tudelft.nl.

Abstract. Limited stroke automatic watch winding poses a challenge due to the proof mass range being smaller than the input displacements. Traditionally the proof mass is connected to the mainspring by a linear reduction transmission however this setup only functions effectively for specific accelerations. This paper proposes to use a nonlinear transmission between the proof mass and the mainspring improve the power output. This transmission will us a singularity to have a mechanical advantage of zero in the middle of its motion range, and increasing the further it moves. This improves the range in which the automatic winding device can operate especially the lower accelerations. A quasi static model of the system is made to estimate the efficiency of the mechanism for different accelerations which is verified by a demonstrator. These efficiencies combined with a human motion analysis suggest it could increase the energy generated to the mainspring by 52% compared to the linear transmission.

Keywords: horology; compliant mechanisms; automatic winding; human motion.

3.1. Introduction

Advances in manufacturing techniques have made it possible to produce compliant mechanisms for watches more easily and allow them to be mass produced at a competitive price. Some great examples are the time setting mechanism of Patek Philippe which replaces the crown of the watch to set the time. The constant escapement of Girard-Perregoux which improves the precision of the watch by compensating for the changing stiffness of the mainspring over its motion range. Or the oscillator of Frederique constant which replaces the whole oscillator assembly including the anchor by a single part. This increases precision of the timekeeping device, decreases the required energy whilst also using less space. This shows that for some mechanisms in a watch it can be very beneficial to make them compliant.

However Automatic winding(AW) mechanisms which use the motion of the wrist to wind the watch have not been made compliant yet. These mechanisms have been around in non-compliant form since the 18th century[1] with different types but have mostly been the rotor type design [2]**.** This mechanism works with an eccentric mass which is allowed to rotate indefinitely around an axis. If the mass rotates it winds the mainspring of the watch via a reduction geartrain. Since Rolex mass produced them first in the 1930's almost all AW mechanisms are based on the same design.

If AW where to be made compliant it cannot have the infinite stoke of the rotor design, thus is has to be of the limited stroke AW design. These function almost the same other than having a limited rotation of the proof mass. However this does make them a lot harder to design, as the force with which the kinetic energy is extracted from the proof mass becomes pivotal for effective operation, and also gives it lower power output potential compared to the rotor type[3].

Furthermore not a lot of information about limited stroke AW is publicly available but there has been a lot of research in energy harvesters(EH) which use a limited stroke. These work on the same

principles as a compliant AW device, a mass is suspended by a spring and damped by a force that stores energy. If this mechanism is then accelerated externally the mass inertia is able to produce power, or in the case of a mechanical watch the mainspring is wound. With EH experiments have been done with varying nonlinear spring stiffnesses[4]–[6] and different transduction mechanisms[7]–[9]. These experiments have shown that both the nonlinear stiffness and transduction mechanism have great effect on the output of such EH and how one should chooses these parameters highly depends upon the input motion. Classically in AW, the mass has been linearly coupled to the mainspring by a reduction transmission, this will be called direct automatic winding(DAW). However this transmission does not have to be linear. So the objective of this paper is finding an alternative nonlinear transmission to improve the energy output compared to DAW.

In section 2.1 the data from[10] is analyzed to create a histogram of the accelerations during walking. In section 2.2 a quasi-static analysis is done to determine the efficiencies of both devices under different accelerations. In section 2.3 the histogram is combined with the quasi static analysis to estimate the power output. In 2.3 a demonstrator is made and tested to prove the theory. In section 3 the results are shown which are discussed in section 4.

3.2. Methods

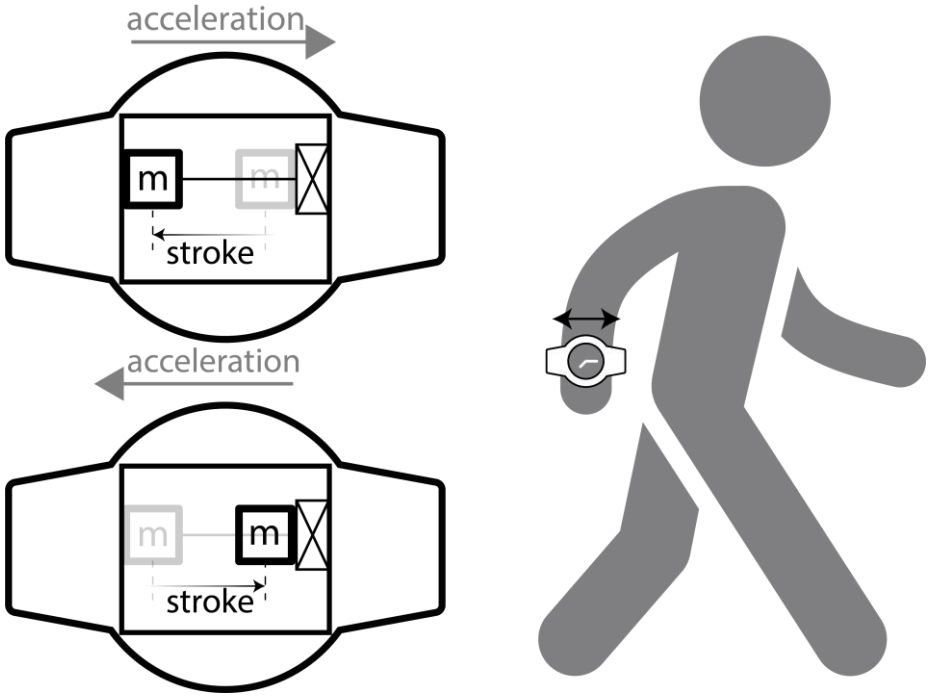

Figure 3.1. automatic winding schematic with acceleration

2.1 human motion analasys

To estimate how an AW mechanism would behave on the human wrist, some analysis must be done on the wrist motion and on the underlying physics of such a mechanism. The winding mechanism in Figure 3.1 shows a proof mass that is able to move linearly, and it is rigidly connected to a mechanism that extracts energy. This mechanism houses the mainspring and the ratchet which allows it to also store this energy. No stiffness is added to the proof mass and the housing as this paper focusses on improving the transmission mechanism from mass to mainspring.

The limited stroke AW device shown in Figure 3.1 can generate power if the acceleration changes direction, and the mass is able to overcome the force imposed by the extraction mechanism and make

a stroke. The intensity of these accelerations combined with the weight and displacement range of the proof mass will determine the maximum available energy E per stroke with the formula:

$$E = m\,d\,a \qquad (1)$$

Where m mass, d stroke length and a the average acceleration of a peak. Which is approximated with the peak acceleration and interpreting it as a sine curve. Thus a will be:

$$a = \frac{2}{\pi} a_{peak} \qquad (2)$$

The weight and internal displacement of an average proof mass in a watch are $m = 20g$ and $d = 10mm$ respectively. For the accelerations the database from [10] is used which contains acceleration data of the human wrist of 8 different subjects doing different activities. This database yields similar results as studies done for the human walking gate like [11], [12]. The displacement axis is chosen in the horizontal plane so gravity has not to be accounted for.

This axis is analyzed by counting the acceleration peaks between 2 zero crossings shown in Figure 3.2 and adding them to a histogram. The peaks will be integrated twice over time to determine their displacement so false peaks with displacements smaller than 50% of the proof mass displacement can be discarded. These probably won't produce any power due to the accelerations being too low or short for the mass to overcome friction or they do not have any meaningful displacement. The residual counts are then evaluated with the formula (1) and (2) described earlier

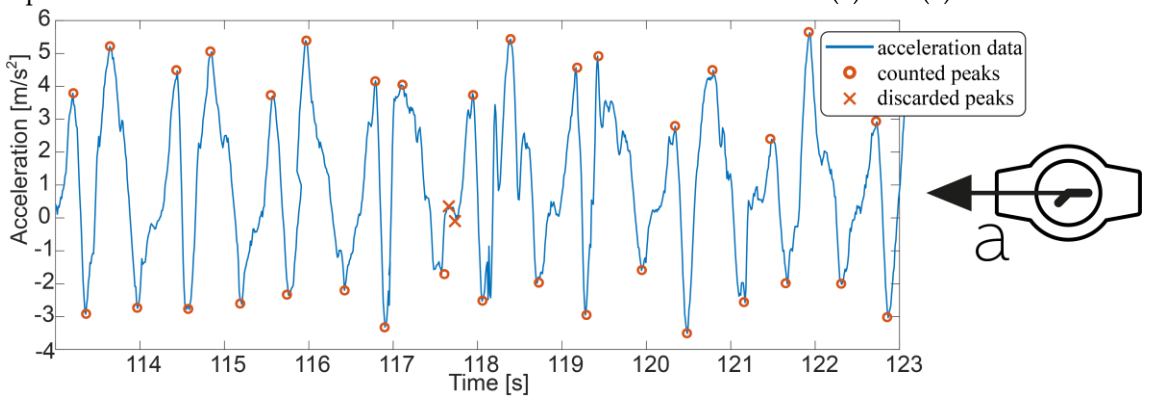

Figure 3.2. acceleration peaks when walking. With counted and discarded peaks

and normalized for time which will give an average power per acceleration. This is shown later in the results.

With the average power per acceleration determined, the total power can be estimated if the efficiency of the transmission mechanisms is known at different accelerations.

2.2 mechanical design

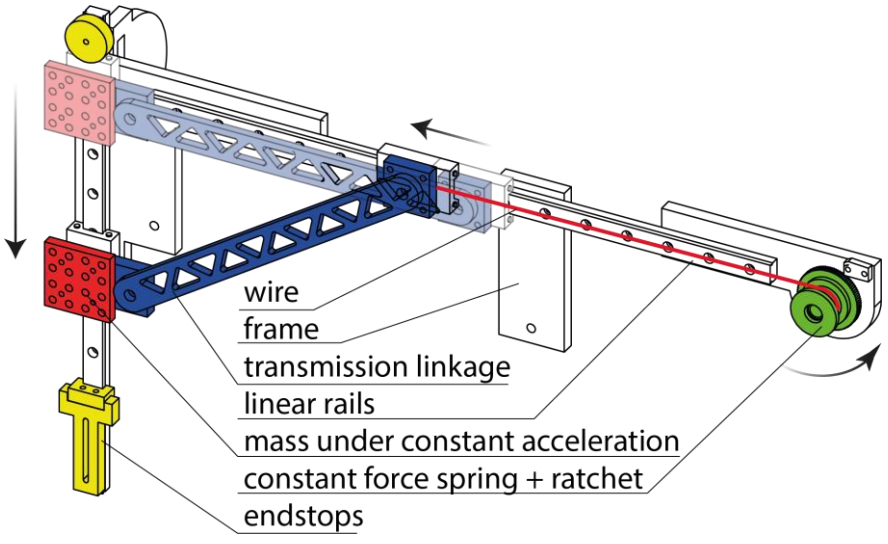

Figure 3.3. *mechanical design of the transmission (PDAW)*

The transmission mechanism will be a period doubling transmission as described in [13]**.** This transmission makes use of a single linkage connected to two linear guides around its singularity position. At the singularity it has zero mechanical advantage, in Figure 3.3 this is will be when the mass is held against its highest end stop. This transmission will increase its mechanical advantage when it moves away from the singularity towards the lower end stop. When the mass is at its maximum displacement the mechanical advantage will be infinite as it has reached a second singularity however the maximum geometrical advantage of this transmission is 1 as it is limited by the length of the beam. In this section a period doubled automatic winding (PDAW) mechanism where the proof mass is connected to the mainspring via this period doubling transmission will be compared to the Direct Automatic Winding (DAW) where the mass is connected directly to the mainspring. This mainspring is a constant force spring which is similar to how watches store their energy normally. The mechanical design of the PDAW is shown in Figure 3.3 with the according mechanical parts. The mechanism will be tested with the use of gravity, by alternating the angle of the linear guide of the mass the acceleration changes. The mass starts at the highest end stop shown in Figure 3.3, and is dropped. This means the winding mechanism is able to make the full stroke. This is comparable to the real world as human input accelerations have displacements which are often 10[BRON] times larger than the internal displacement of the proof mass.

This specific transmission was chosen to be useful because of two reasons. The first due to its double sided operation. The period doubling effect of the transmission the PDAW will also function as a reversal mechanism. The mechanical design shown in figure 3.3 only shows one side of the mechanism, if the vertical linear guide is lengthened on top. It will allow for double sided operation.

But the second and most important reason is due to the fact that energy harvesters have to maximize their *work* [14] of the proof mass to allow for maximum energy to be extracted. With the DAW shown in Figure 3.4(A) this is the case when the acceleration force is equal to extraction force. However, if the acceleration force is lower the mass will not move and no energy will be stored. If the acceleration is higher the mass will hit the end of the stroke with residual kinetic energy which will then be dissipated. Thus the force component was not optimal.

With the PDAW in Figure 3.4(B) this force is nonlinear allowing for both higher and lower input accelerations to be captured as shown in figure 3.4 (D). Where two regions are marked when the input acceleration changes. This figure also shows that when the acceleration is lower, the displacement goes down. Thus decreasing the efficiency at these accelerations.

3.2.2 analytic model

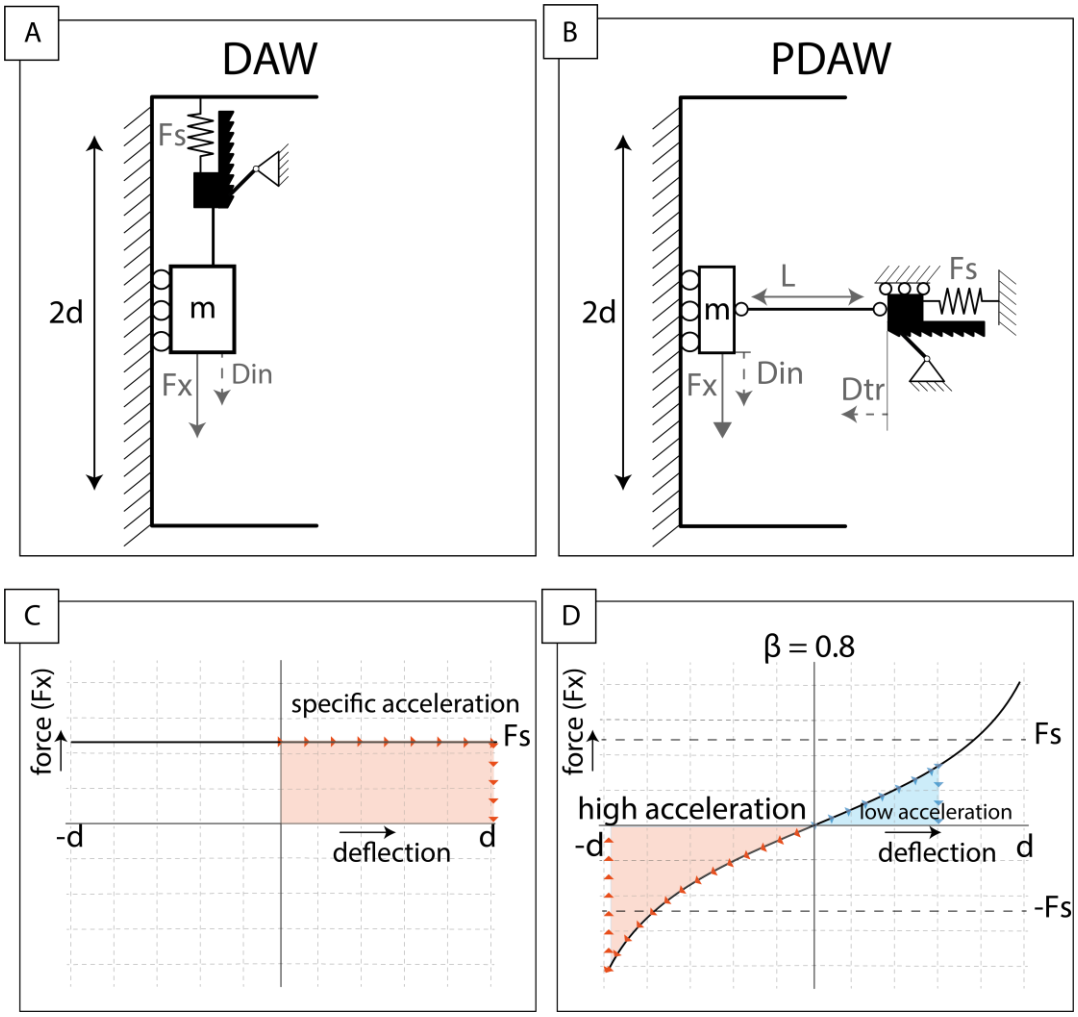

Figure 3.4. *(A) The DAW system with the inertial mass A directly coupled to the spring with constant force Fs (B)the PDAW system with the inertial mass m coupled via a linkage to the spring with constant force fs. Both have displacement range 2d (C) shows force f_x acting on the mass from the DAW with a single stroke. (D) shows force f_x acting on the mass of the PDAW through its operating range. It also shows how it would respond to a high and low input motion. The area depicted under the graph is the energy stored of a stroke.*

The theoretical mechanism of the DAW and PDAW is shown Figure 3.4(A) and Figure 3.4(B) respectively. The ratchet is assumed to have infinite teeth and the mass is modeled as a point mass. In Figure 3.4(C) and Figure 3.4(D) the force (F_x) the proof mass experiences from the spring F_s is shown. The amount of energy it stores can be estimated by calculating the area under the force deflection graph.

The efficiency of these devices can be estimated by an analytical model. The starting situation is depicted in Figure 3.4(A) and Figure 3.4(B) with the inertial mass in the middle of its motion range. Then the mass is released under a constant acceleration. The spring with constant force F_s cannot return any energy to the system due to the ratchet. Thus the position where the proof mass will come to rest will be the energy equilibrium of the spring and the mass. So first the energy stored in the spring must be determined, For the DAW this is:

$$E_{s1}(D_{in}) = F_s D_{in} \quad (3)$$

Where E_{s1} is the energy stored in the spring, F_s is the force of the constant force spring and D_{in} is the displacement of the proof mass also shown in Figure 3.4(A). The energy stored in the PDAW is again dependent on the displacement of the spring.

$$E_{s2} = F_s D_{tr} \quad (4)$$

Where E_{s2} is the energy stored in the PDAW spring, F_s is the force of the constant force spring D_{tr} is the extension of the constant force spring. D_{tr} is correlated with the proof mass displacement D_{in} via the Pythagoras theorem where:

$$D_{tr} = L - \sqrt{L^2 - D_{in}2} \quad (5)$$

Where L is the length of the linkage. Substituting (2) and (3) gives the energy stored in the PDAW:

$$E_{s2}(D_{in}) = Fs * (L - \sqrt{L^2 - D_{in}2}) \quad (6)$$

The potential energy due to the input acceleration is:

$$E_a(D_{in}) = ma_{in}D_{in} \quad (7)$$

Where E_a is the potential energy, m the mass, a_{in} the input acceleration and d_{in} the proof mass displacement. If the mass moves is also dependent on the derivative of the potential energy, This will determine when the DAW will start to move and when not.

$$dEs<dEa \quad \textit{mass will move} \quad (8)$$

$$dEs>dEa \quad \textit{mass will not move} \quad (9)$$

$$E_a(Din) = E_{s1,s2}(Din) \quad (10)$$

To compare both systems two design parameters are taken into consideration, $\alpha = F_s/F_a$ which is the spring force f_s divided by the inertial force of the mass f_a. This is a dimensionless value which can be used to determine the efficiency of the mechanism per acceleration, independently of scale and mass.

The second parameter is $\beta = d/l$ this defines the nonlinearity of the PDAW. This is the displacement range of the proof d mass over the length of the transmission rod L. This value has a maximum of 1 as the range of motion of the proof mas cannot exceed the length of the connecting rod. It is assumed when the mass hits the end stop all remaining kinetic energy will be dissipated. This is done to show the influence of the PDAW not the influence of the coefficient of restitution of the mass. The efficiency of the winding device can be calculated by dividing the energy stored in the spring by the maximum available work of the stroke.

$$\mu = \frac{E_{spring}}{E_a(d)} \quad (11)$$

If we then substitute (3),(7),(10) and (11) we get for the DAW:

$$\boldsymbol{\mu_{s1}} = \begin{cases} \boldsymbol{\alpha} & \boldsymbol{0 < \alpha < 1} \\ \boldsymbol{0} & \alpha > 1 \end{cases} \quad (12)$$

The bound is where the acceleration becomes lower than the spring stiffness, here the mass will not move. Thus not storing any energy. If the acceleration just slightly higher the proof mass will hit the end stop, thus dissipating energy. The efficiency is shown in Figure 3.7(A) in the next section.

If we substitute (6), (7), (10) and (11) the efficiency of the PDAW is:

$$\boldsymbol{\mu_{s2}} = \begin{cases} \dfrac{\boldsymbol{2}}{\boldsymbol{\beta} * \boldsymbol{\alpha} + \dfrac{\boldsymbol{\beta}}{\boldsymbol{\alpha}}} & \boldsymbol{\beta < \dfrac{2}{\alpha + \dfrac{1}{\alpha}}} \\ \dfrac{\boldsymbol{\alpha}}{\boldsymbol{\beta}}(\boldsymbol{1 - \sqrt{1 - \beta^2}}) & \beta > \dfrac{2}{\alpha + \dfrac{1}{\alpha}} \end{cases} \quad (13)$$

The bounds again are where the proof mass hits the end stop of the AW device. But in the PDAW this is dependent on both the α and β. The efficiency of this mechanism is plotted in Figure 3.7(B) in the next section.

2.3 power output

Using the power histogram from human motion Figure 3.5(A), combined with (11) and (12) gives a power output for the mechanisms. With the mass 20g and displacment 10mm with the, F_v can be optimized by a line search for optimal power. F_s will determine the efficiency of the mechanisms over the acceleration range which can then be used to calculate the power output histogram of both the DAW and PDAW which are shown in Figure 3.5(B) and Figure 3.5(C) respectively. Taking the sum of this histogram gives an avarage power of both devices which is .56 mW for the DAW and .86mW for the PDAW. This is an 52% increase for the PDAW. This isncrease is mostly due to the fact that the PDAW can handle bot high and low accelerations, with the DAW the cutoff amplitude is clearly visible as for lower accelerations the power output is zero.

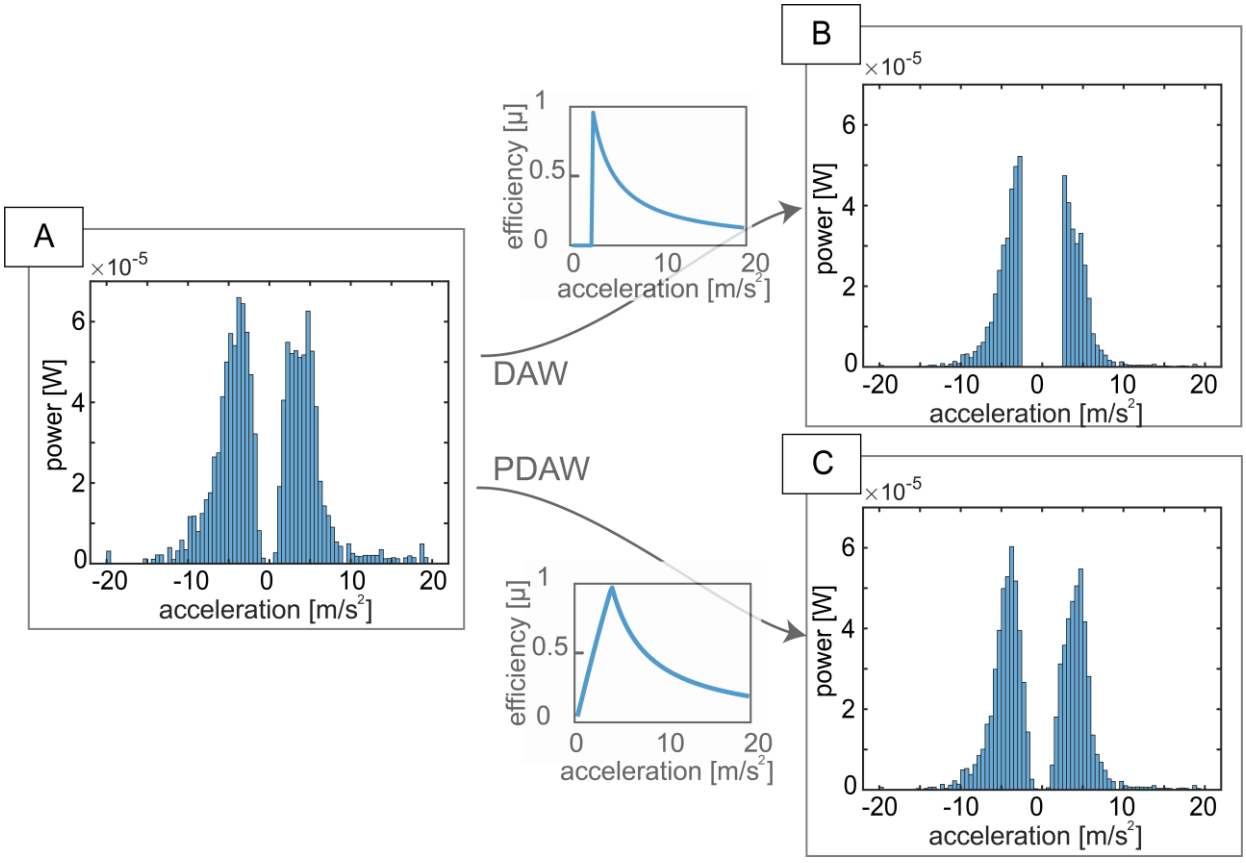

Figure 3.5. (A)Power histogram for human walking motion. (B) power histogram for the DAW after the efficiency is taken into account (C) Power histogram for the PDAW after the efficiency is taken into account.

3.2.4 demopnstrator setup

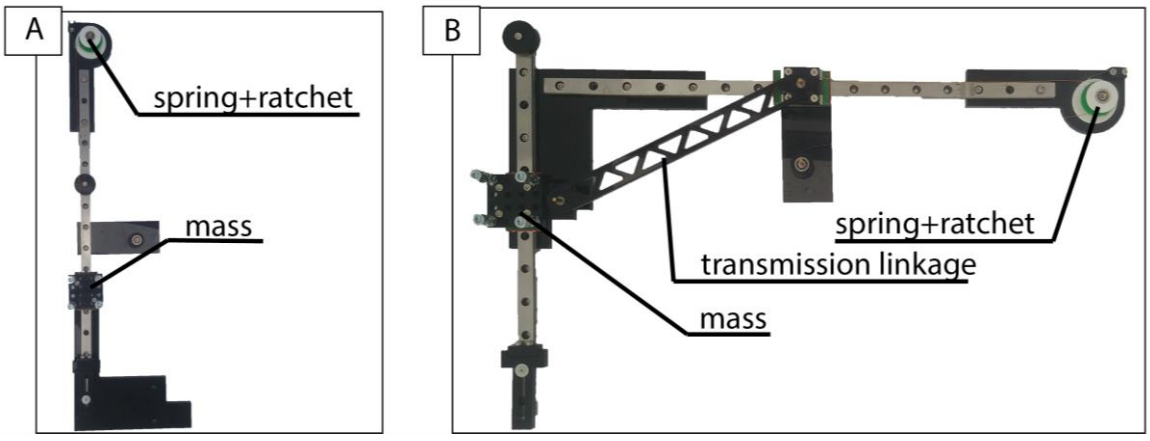

Figure 3.6. *experimental setup.(A)DAW (B)PDAW*

Testing the mechanism was done by angling it in the gravitational field to represent different input accelerations. The mass was then held at height d against a block, from there it was dropped to see how far the spring was wound. This quasi static test will verify the theoretical efficiency described in section 2.2.

3.3. Results

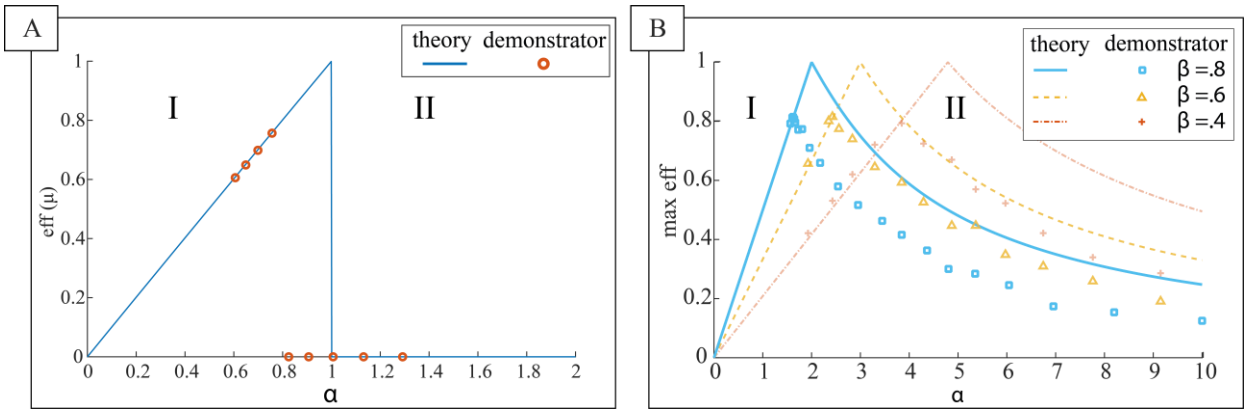

Figure 3.7. (A) efficiency of the directly coupled winding device. with operating regime I and II. (B) efficiency of the winding device with the transmission. with operating regime III and IV.

In Figure 3.7 the efficiencies of both mechanisms are shown on the vertical axis and α on the horizontal axis. With low α being high accelerations and high α being low accelerations relative to the force of the spring. It can be seen in Figure 3.7(A) that with the DAW there is one regime where it operates and one where it does not. Operating regime I where the DAW generates power which increases slightly with increasing accelerations. And regime II where the proof mass does not move thus not generating any power.

The efficiency graph in Figure 3.7(B) shows the efficiency of PDAW with $d/l = .8$ and varying input acceleration compared to the stiffness of the mainspring n_a. Here two operating regimes can be seen III and IV. In operating regime IV the displacement of the proof mass depends on the input acceleration. In operating regime III the proof mass hits the end stop and dissipates energy.

The measured data from the experiments show us that both mechanisms show the same operating regimes as in the analytic model of the system. However they do so at reduced efficiency as a whole.

3.4. Discussion

For the DAW mass in Figure 3.7(A) operating regime I is where the winding device produces power. It behaves efficiently when $\frac{f_v}{f_a}$ is near 1. Efficiency decreases when the input acceleration force increases. This means when a higher acceleration is applied the proof mass hits the end stop of the motion range, which loses a lot of energy. Thus decreasing overall efficiency.

In regime II of the DAW, where no power is generated. Means that the acceleration force is lower than the force exerted by the spring. This means the mass can't move, and not store any energy. Thus there is a clear cutoff amplitude where the AW will stop working.

Operating regime I For the PDAW is similar to regime I of the DAW. The difference is that in the DAW dE_s is smaller than dE_a over the whole displacement range. Whilst for the PDAW the dE_s is dependent on displacement of the mass and in the end it is larger then dE_a. This determines where on the stroke it stores most of its energy.

In regime II the PDAW makes the biggest difference compared to the DAW. Due to the mechanical advantage being 0 in the middle of its operating range the proof mass will still move at very low input accelerations. As the input acceleration increases the range in which the proof mass moves increases. this increases the efficiency until maximum efficiency is reached when the potential energy due to the acceleration is equal to the maximum energy that can be stored in one stroke.

This theory was then verified by making a demonstrator and testing it. The spring extension was measured using a ruler on top of the setup shown in Figure 3.6. The precision of the ruler was deemed enough due to the fact that the ratchet wheel on the spring had 90 teeth, which limits the precision of the measurement to be .6mm of spring extension, which can easily be read from the ruler. If more teeth where used on the ratchet wheel, a more accurate measuring device would be needed.

The measurements of the mechanism clearly showed a decrease in power compared to the theoretical quasi static analysis. This is due to the friction in the bearings and the ratchet mechanism. This friction gives a decrease in efficiency of about 20%. This percentage counts for this specific test mechanism however. If the mechanism is made compliant or built another way, this could be a different value.

In the section 2.3 the decrease in efficiency by friction is not yet taken into account. This means that the cutoff amplitude for the DAW is 20% lower and the optimal power peak for the PDAW shifts by 20% as well. This decreases the power output of the both mechanisms by about 20%, but it should also be taken into account when optimizing for f_s, as this displaces the optimal acceleration peak because more force is required to move the mass.

The β proved to be not as important for two reasons. One, a change in the β could be compensated with an increase in mainspring stiffness thus the peak shown in Figure 3.7(B) could still be placed on the right spot. Two, the main increase in power compared to the DAW comes from the lower accelerations which works almost the same for high and low values of β. Theoretically the most optimal solution would still be an β of 1. This would generate the highest displacements for the largest acceleration range as all of the energy would be stored at the end of the stroke. However in the real world this will most likely not be feasible as this would bring the gear ratio at the end of its stroke to infinity. This will create massive stresses on the mechanism and create large rotation angles of hinges. Which will make it difficult to make it compliant. Taking a lower βwould be more practical at a slight decrease in power output.

The increased power was calculated with both masses being equal. However having a transmission might not increase the volume efficiency as the transmission does take up space which could otherwise be used for increasing the mass. However by having the PDAW there is no need for a reversal mechanism and the ratchet mechanism can be included in the design making it more volume efficient again. If this would eventually lead to a total increase or decrease in power output is highly dependent on the design and person that would be wearing the device. If the transmission does not change the proof mass weight the best choice will still be the PDAW as this it is more flexible in the different motions it can handle. Thus making it a more robust power supply.

This proves that changing the linear transmission between the proof mass and mainspring to a nonlinear period doubling transmission can increase the power output of limited stroke AW for human walking motion. Further optimization still has to be done on the orientation of the device relative to the watch, the stiffness of the suspension and seeing how it would fit in a watch with accompanying mechanisms.

3.4.2 Recommendations

1. see if this can also be applied to energy harvesters, where a nonlinear transmission can be used between the transduction mechanism and the proof mass. This could yield an increase in power output especially in situations where input accelerations are less predictable in fields like wave energy, vehicle suspension or again human motion

2. This paper considered the situation where the mass is suspended by zero stiffness. In the future this transmission should be combined with varying stiffnesses or gravity balanced stiffness to make the mechanism more robust and improve output.

3. More activities could be taken into account so an optimization can be done on the average activity of a human. This can tell something about what the optimal orientation will be and might yield different results in the optimization of f_s.

3.5. Conclusion

We have analyzed the human walking motion to see how much power is available for an AW device on the wrist in a single axis. This was done by making a histogram of how many strokes such a mechanism can make under different accelerations. A comparison was done between a more classical limited stroke AW and a newly proposed design with a nonlinear transmission between the proof mass and the mainspring. The performance of this design on input acceleration was verified with a demonstrator. With this information it is shown that the PDAW is a viable option for limited stroke automatic winding. The increased power is highly dependable on orientation and activity but the analysis showed the output could increase up to 52%. This showed that by adding a nonlinear transmission between the proof mass and the mainspring the power output of the AW device can be changed and even improved.

References

[1] J.-C. Sabrier, *The Self-Winding Watch*, Éditions C. paris, 2011.

[2] M. Cheong Lei, L. Xie, and R. Du, "Kinematic analysis of an auto-winding system with the pawl-lever mechanism and its application in energy harvesting," *Int. J. Mech. Sci.*, vol. 52, no. 12, pp. 1605–1612, 2010, doi: 10.1016/j.ijmecsci.2010.08.001.

[3] E. M. Yeatman, "Energy harvesting from motion using rotating and gyroscopic proof masses," vol. 222, pp. 27–36, 2007, doi: 10.1243/09544062JMES701.

[4] S. P. Pellegrini, N. Tolou, and M. Schenk, "Bistable vibration energy harvesters : A review," vol. 24, no. 11, pp. 1303–1312, 2012, doi: 10.1177/1045389X12444940.

[5] S. Zhou, J. Cao, D. J. Inman, J. Lin, S. Liu, and Z. Wang, "Broadband tristable energy harvester: Modeling and experiment verification," *Appl. Energy*, vol. 133, pp. 33–39, 2014, doi: 10.1016/j.apenergy.2014.07.077.

[6] R. R. M. J. Brennan and B. R. M. I. Kovacic, "Potential benefits of a non-linear stiffness in an energy harvesting device," pp. 545–558, 2010, doi: 10.1007/s11071-009-9561-5.

[7] P. D. Mitcheson, T. C. Green, E. M. Yeatman, and A. S. Holmes, "Architectures for vibration-driven micropower generators," *J. Microelectromechanical Syst.*, vol. 13, no. 3, pp. 429–440,

2004, doi: 10.1109/JMEMS.2004.830151.

[8] T. Von Büren, P. D. Mitcheson, T. C. Green, E. M. Yeatman, A. S. Holmes, and G. Tröster, "Optimization of Inertial Micropower Generators for Human Walking Motion," vol. 6, no. 1, pp. 28–38, 2006.

[9] P. Pillatsch, E. M. Yeatman, and A. S. Holmes, "A piezoelectric frequency up-converting energy harvester with rotating proof mass for human body applications," *Sensors Actuators, A Phys.*, vol. 206, pp. 178–185, 2014, doi: 10.1016/j.sna.2013.10.003.

[10] A. Reiss, "Personalized Mobile Physical Activity Monitoring for Everyday Life Attila Reiss," no. January, 2014.

[11] J. J. Kavanagh, R. S. Barrett, and S. Morrison, "Upper body accelerations during walking in healthy young and elderly men," *Gait Posture*, vol. 20, no. 3, pp. 291–298, 2004, doi: 10.1016/j.gaitpost.2003.10.004.

[12] P. Arnell, *The Biomechanics and Motor Control of Human Gait*, vol. 74, no. 2. 1988.

[13] D. Farhadi Machekposhti, *Compliant transmission meChanisms*. 2019.

[14] A. H. Hosseinloo and K. Turitsyn, "Fundamental Limits to Nonlinear Energy Harvesting," vol. 064009, pp. 1–8, 2015, doi: 10.1103/PhysRevApplied.4.064009.

4 Conclusion

The goal of the research was improving compliant automatic watch winding. Making automatic winding compliant in and of itself will create limitations on the performance of the mechanism. The limitations will be due to limited motion range of the proof mass, stiffness of the suspension and the effect of gravity coming into play when using a limited stroke winding device. I chose to focus on a single of these limitations which is the limited motion range of the mass. For that I proposed a novel concept of using a nonlinear transmission, to see if it could increase the power transmitted to the barrel spring. In this study it was found that a nonlinear transmission from proof mass to barrel spring could increase the power output of limited stroke automatic watch winding on human motion. It was shown that using the nonlinear transmission the device could use a wider range of input amplitudes. Where an analyses of the human walking gate showed a possible increase in power of about 50% compared to a classic reduction gear. It does this by using single linkage to create a period doubling effect with the added benefit of double sided operation. This has a low transmission ratio in the middle of its motion range, and an increasing transmission ratio the further it moves from the middle. The study gave good insight in what transmission ratio should be used for a specific barrel stiffness.

4.1 Limitations and recommendations

Apart from the increase of power in the limited stroke automatic winding, still a lot of work has to be done to make it a working mechanism. And there are a few limitations to the approach. One of the limitations is that the ratchet was modeled with infinite teeth. If this is taken into account it will make the efficiency of the mechanism lower. Now it was modeled as a ratchet wheel with infinite teeth so it does not have any backlash. In the real world however backlash of the ratchet will give energy back to the proof mass and not store it in the barrel spring. The study was however done by comparing it to a normal reduction gear which will also be effected by this, thus it can still be said that the nonlinear transmission will have better performance. Another limitation is not taking into account the volume efficiency of the mechanism. The comparison was done by starting with the same range of motion and same weight. This was done to ensure a fair comparison between using two separate transmissions. The nonlinear transmission will however take up more space in the watch making the volume efficiency lower. By how much however is difficult to say as it depends on how the watch will be designed in the first place as the nonlinear transmission will have more design freedom in the watch itself. Also the nonlinear transmission functions as a reversal mechanism which still has to be built in to the watch when a normal reduction transmission is used. Only when the design is developed further and all functionalities are taken into account this can be determined. To move forward in making this into a working mechanism two steps definitely have to be taken. Firstly Creating a hybrid mechanical compliant where the mass is suspended by a mechanical hinge and the transmission is compliant. Which should be built with more professional manufacturing equipment to create the precision needed to test it. It should be tested on a motion stage with a range of motion comparable to the human wrist. To see if the theory works in the real world, and also to see if the transmission can cope with the forces. The second step is seeing it the mass suspension can be made compliant by creating a very low stiffness suspension spring in a very confined space. This must be done in tandem with analysing human wrist motion to see at what angle the mechanism must be installed in the watch, as the angle will also determine how much the stiffness must compensate for gravity. This will be quite complex to do, but not impossible. All this combined can possibly make an automatic winding device that can outperform the mechanical rotor mechanism found in most watches today. As this does not rely on the random motion of the human wrist but on more predictable motion like walking.

5 Summary

Classic automatic winding of watches is based upon a rotor making a full circle. This combined with a ratchet mechanism and a reduction gear allows it to store energy in the barrel spring. This allows the watch keep on running long as it has enough external motion. The rotor type design is really effective at doing this as it has an infinite motion range. This allows it to store all potential energy in the form of kinetic energy which will then over time be converted to elastic energy in the mainspring. This kinetic energy buffer makes it effective for both high and low input accelerations. If the motion range was limited this would not be possible as all the energy in an input motion needs to be captured in the mainspring immediately. If it does not, the mass will hit the end of its motion range with remaining kinetic energy which will be mostly lost. This loss of energy makes limited stroke mechanisms less efficient. Limited stroke can have advantages however. One of the advantages is giving more design freedom in the watch itself, as this mechanism does not need the rotational point to be in the middle of the watch. It also allows the mechanism to be made compliant which reduces wear on parts, and could simplify the whole automatic winding mechanism. In this study I tried to address one of the main drawbacks of limited stroke automatic winding which is that it cannot deal well with varying accelerations. For this I proposed using a nonlinear transmission from the proof mass to the mainspring. This transmission would make it more effective for varying input accelerations. The transmission would be a frequency doubling transmission created by using a single linkage in its singularity position. This will create a transmission with a transmission ratio of zero in the middle of the motion range, and increasing the further you move either direction. The efficiency of such am mechanism was analysed and measured with a demonstrator by applying different accelerations. These efficiencies where then used to determine how it would perform on the human wrist whilst walking. This showed a possible increase of 50% in transmitted power the case considered and gave insight in how the mechanism should be dimensioned compared to the stiffness of the mainspring.

6 Appendix

6.1 limited stroke automatic winding

the literature review on energy harvesting gave insight in what makes inertial energy harvester efficient ant how the proof mass should behave on different inputs. In energy harvesting there are different kinds of harvesters, where most of them are focussed on harmonics. With human motion however there is only a few activities where harmonics could come into play. This combined with the fact that everyone moves different makes harmonics not a viable solution. On nonharmonic energy harvesting less research has been done. Harvesters which use more sporadic input motion are less researched, but the research that has been done shows clearly what could make It work efficiently. A basic inertial energy harvester consists of tree parts. The mass the spring and the damper. The combination of the three determines how well the harvester works in the intended motion. The harvester extracts maximum energy when it maximizes the internal work of the proof mass. Let's take some theoretical input accelerations, with different strengths and durations to show this. These accelerations will be imposed upon a basic energy harvester consisting of a proof mass connected to an energy extraction mechanism. Every acceleration contains different amounts of energy combined with a different acceleration. There are two problems with this limited stroke AW device. The first is that the displacement of the input acceleration is larger than the internal displacement of the proof mass. Which means the AW device will most likely not use the whole duration of the acceleration before hitting the end of the stroke. Thus the mechanism is limited by its internal displacement. Thus the maximum work will be the extraction force* internal displacement. The second problem is the changing acceleration. this means that when the extraction force is constant, it only works optimally for a single acceleration. If the acceleration is any higher it will decrease in efficiency. If it is any lower it will stop working as a whole. With electrical transduction mechanisms this extraction force can be altered by changing the electrical circuit behind it, or changing to a different transduction mechanism. This can also be actively done whilst the mechanism is in use. Mechanically this hasn't been done yet. Actively changing the Extraction force by a mechanical mechanism will be difficult to do. However using a nonlinear transmission will be possible.

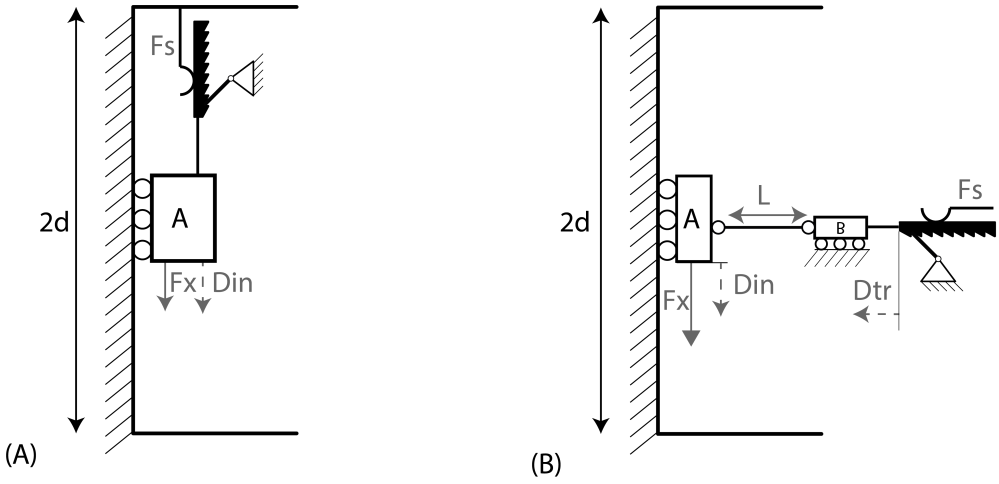

Figure 6.1: **DAW and PDAW**

figure 6.36 shows the mechanism witht a direct connection to the barrel spring. and also the nonlinear transmission proposed.

The transmission mechanism will be a period doubling transmission as described in [DAVOOD]. This transmission makes use of a single linkage connected to two linear guides around its singularity position. At the singularity it has zero mechanical advantage, in Figure 3 this is will be when the mass is held against its highest end stop. This transmission will increase its mechanical advantage when it moves away from the singularity towards the lower end stop. When the mass is at its maximum displacement the mechanical advantage will be infinite as it has reached a second singularity however the maximum geometrical advantage of this transmission is 1 as it is limited by the length of the beam. In this section a period doubled automatic winding (PDAW) mechanism where the proof mass is connected to the mainspring via this period doubling transmission will be compared to the Direct Automatic Winding (DAW) where the mass is connected directly to the mainspring. This mainspring is a constant force spring which is similar to how watches store their energy normally. The mechanical design of the PDAW is shown in Figure 3 with the according mechanical parts. The mechanism will be tested with the use of gravity, by alternating the angle of the linear guide of the mass the acceleration changes. The mass starts at the highest end stop shown in Figure 3, and is dropped. This means the winding mechanism is able to make the full stroke. This is comparable to the real world as human input accelerations have displacements which are often 10[BRON] times larger than the internal displacement of the proof mass. This specific transmission was chosen to be useful because of two reasons. The first due to its double sided operation. The period doubling effect of the transmission the PDAW will also function as a reversal mechanism. The mechanical design shown in figure 3 only shows one side of the mechanism, if the vertical linear guide is lengthened on top. It will allow for double sided operation. But the second and most important reason is due to the fact that energy harvesters have to maximize their work [14] of the proof mass to allow for maximum energy to be extracted. With the DAW shown in Figure 4(A) this is the case when the acceleration force is equal to extraction force. However, if the acceleration force is lower the mass will not move and no energy will be stored. If the acceleration is higher the mass will hit the end of the stroke with residual kinetic energy which will then be dissipated. Thus the force component was not optimal. With the PDAW in Figure 4(B) this force is nonlinear allowing for both higher and lower input accelerations to be captured as shown in figure 4 (D). Where two regions are marked when the input acceleration changes. This figure also shows that when the acceleration is lower, the displacement goes down. Thus decreasing the efficiency at these accelerations. To find out if this mechanism would outperform the direct connected mechanism. I first started to make a numerical model which would later need to be verified by using the AW device on a shaker.

6.2 Numerical model and shaker verification

6.2.1 prototype and numerical model

This section explores the first prototype tests and the corresponding numerical model, it shows the problems I had with the first setup and what i learned from it to comceptualize the second setup. To proof the mechanism.

6.2.2 first prototype

To verify the model a prototype had to be made and put on the shaker. First the DAW was made to learn how it would be made and also to verify the model without any nonlinear transmission. This consisted of a hammer type mass and a rotating ratchet wheel. This ratchet wheel wound up a wire which was connected to a mass which can will be lifted for when the proof mass oscillates. The mass is there as a substitute for the barrel spring of a watch. to give a constant force.

In appendix 1 the measurements and numerical model for the DAW is shown. This shows the model followed the prototype quite accurately. In the appendix the green and red lines are the amount of energy the mechanism stores. If the lines stay close the model accurately predicts the power of

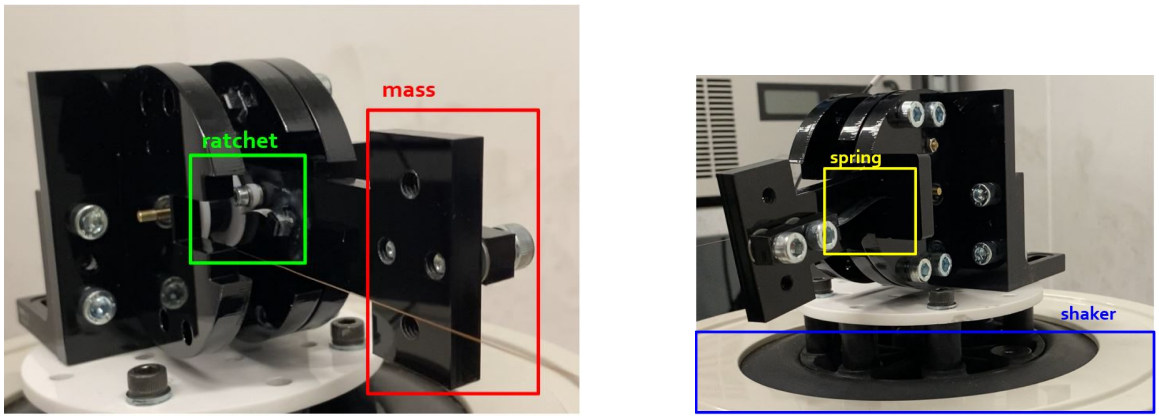

(a) left view **(b)** right view

Figure 6.2: **DAW prototype**

the prototype. This first prototype did show us one of the problems of the mechanism. One of the problems was gravity, this would mean the mass was almost always at the lowest end-stop which is undesirable when measuring. This was easily neglected by rotating the mechanism 90 degrees. The other was using the mass as a substitute for the constant force spring. As the mass has more inertia compared to a constant force spring. Also the mass had to be hanged from a separate structure as it could not be mounted to the shaker. The setup this way was not infinitely stiff. Thus when the mass was lifted, it showed a clear delay compared to the proof mass pulling the lifting wire. Thus the force experienced by the proof mass could not be guaranteed. This meant replacing the mass with a constant force spring.

6.2.3 second prototype

The second prototype had the improvements proposed before. Having a constant force spring and faced horizontally. It was designed to House both the DAW mechanism and the PDAW mechanism. So both mechanisms could be measured under similar circumstances. Both transmissons mounted to the prototype are shown in 6.14 and 6.3

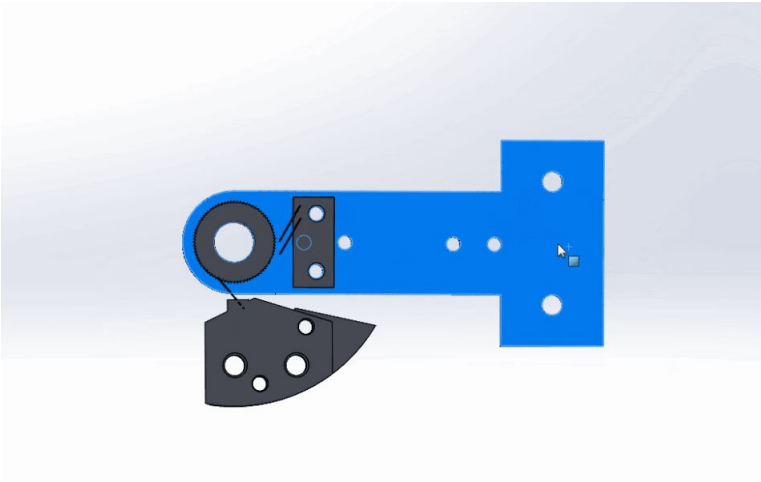

Figure 6.3: **DAW transmission**

6.2.4 prototype PDAW

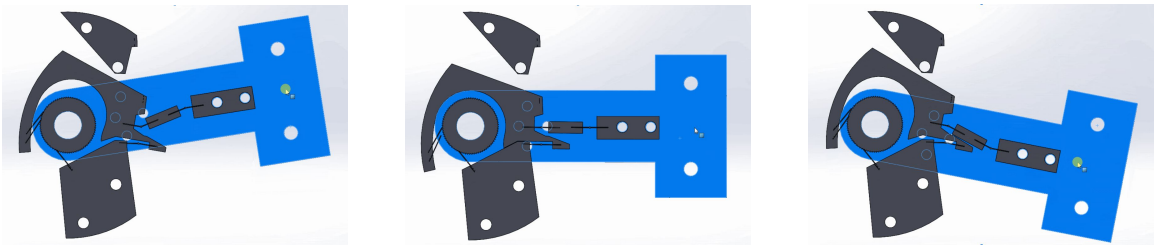

(a) up **(b)** mid **(c)** down

Figure 6.4: **PDAW transmission prototype with motion**

These mechanisms wehere mounted to the hammer like shown in figure 6.5 and the full setup mounted to the shaker on figure 6.6. Here also the lasers are visible to measure extension of the constant force spring and the position of the hammer during shaking. This was necessary to see is the prototype would follow the simulation.

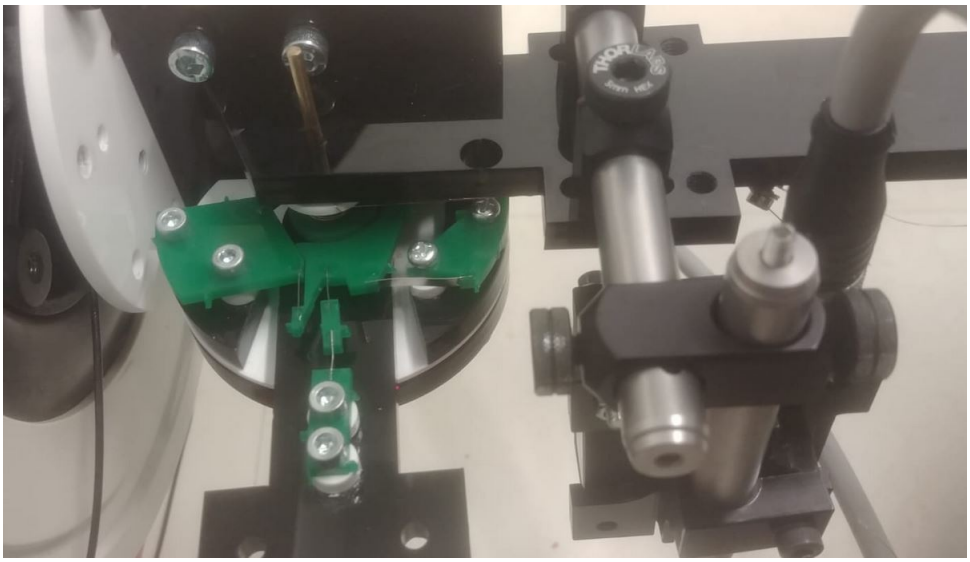

Figure 6.5: **mounted PDAW transmission to prototype**

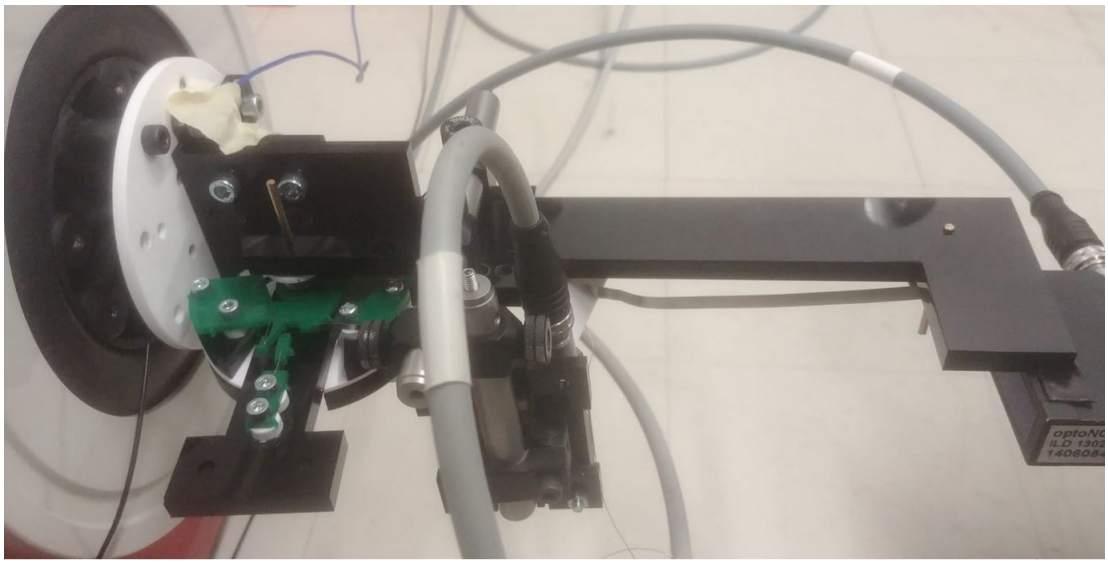

Figure 6.6: **full measurement setup of PDAW**

Running the shaker at different accelerations will show hot much power it will store when operating. This gave us the graph shown in figure 6.7. This is the shaker running at 5 Hz with changing accelerations. The PDAW transmission clearly shows a higher maximum output of the mechanism at large accelerations. And the DAW shows clear dropoff of power generation at .6G. this is the point where the DAW gets saturated. There where however problems with the test. The first and most important one was the motion range of the shaker. The motion range of the shaker at 1G was as large as the motion range of the automatic winding device. So when the acceleration became lower, the winding device was not able to make the full stroke. As the input displacement becomes too little. This makes the results limited by input displacements, not by the limitations of the device itself. Next to that both mechanisms where quite fiddly sometimes they worked well, and the next test they worked bad again. Especially the PDAW was very sensitive to the friction fore of the ratchet when freewheeling. As the transmission increases the friction force acting o the proof mass. It was impossible to get the same result every time. The operation of the PDAW is shown in section 5.2 There the energy it produces is shown as well as the prediction of the model. With the measurements of the prototype it is clearly visible when the acceleration reaches a point where the proof mass starts jumping an extra tooth. That is the point there the slope of the energy stored over time changes angle. In figure 6.7 we can however see the acceleration where the DAW stops producing more power, as at this point it is saturated.

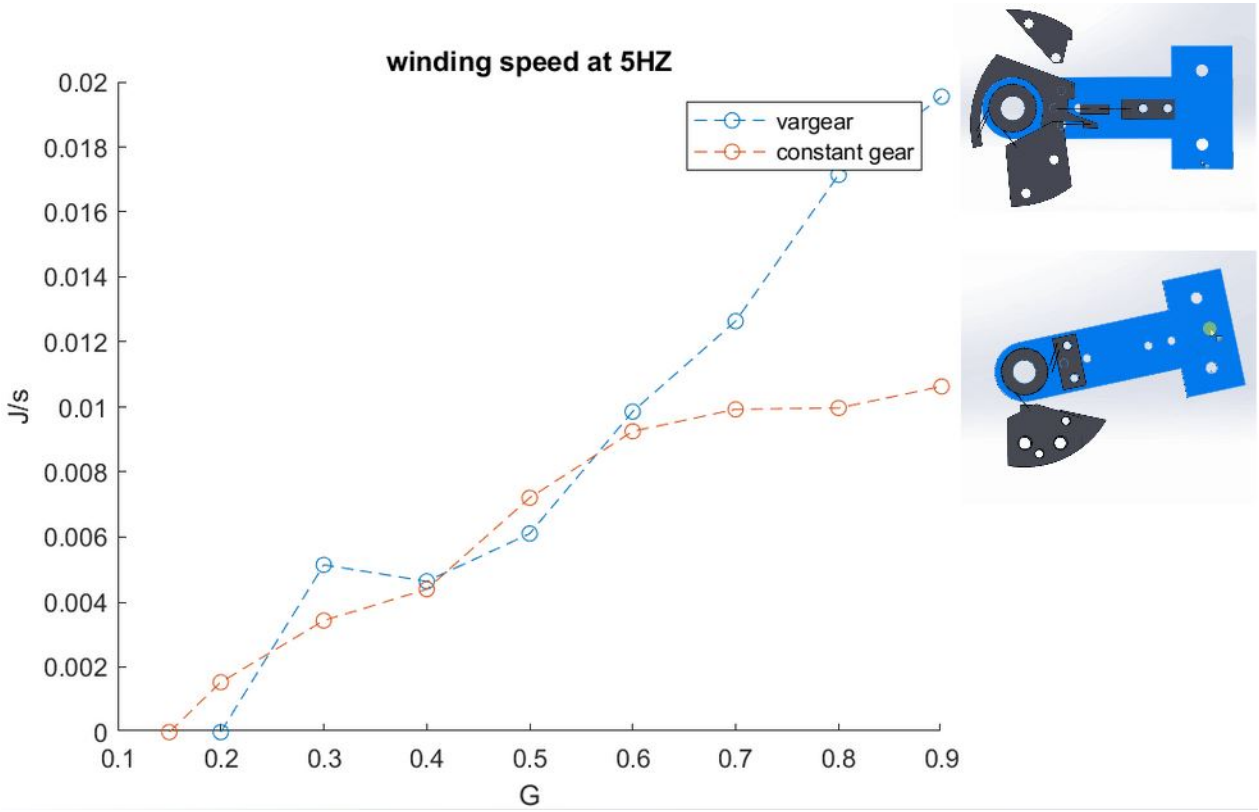

Figure 6.7: **power output of the prototype with different transmissions**

The tests showed the mechanism could be built, and be made functional. However the mechanism cannot be made consistent, due to the fact that the production method and quality is not sufficient.

6.2.5 Numerical model AW

mass

The numerical model is built up in different blocks. With the dynamics added step by step we start off with a differential equation of just the mass. then the differential equation is expanded by adding a suspension spring:

FORMULA

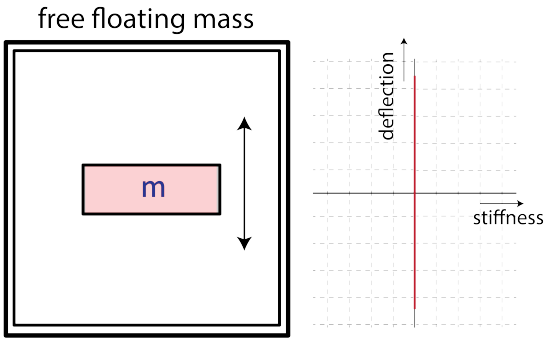

Figure 6.8: **mass**

mass spring

The spring is added as a normal spring with the force depending on displacement and having a constant stiffness.

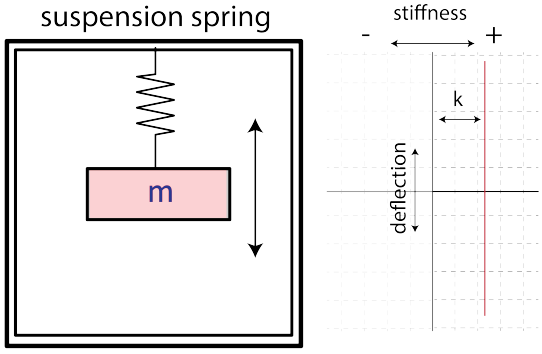

Figure 6.9: **mass spring system**

mass damper

Then a liittle damping is added to stabilize the numerical model.

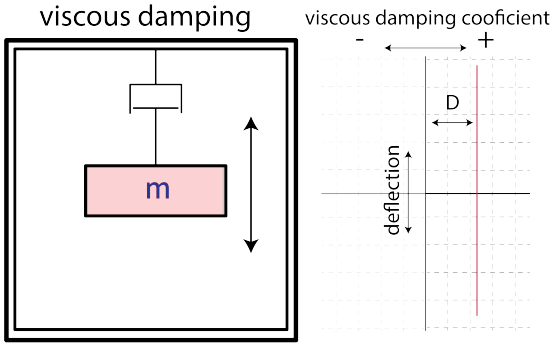

Figure 6.10: **mass damper system**

endstop

Then the endstops of the proof mass are added. These end-stops are essentially a section where the stiffness of the mechanism increases by a very large amount. So they where made with the use of a tanh() function to create a step to a very high stiffness. The internal function of matlab with the eventfunction did not give a stable result as sometimes the mass would fall trough the endstops. Doing it this way makes the simulation slower however as the nonlinear function makes solvint the differential equation difficult. For that reason the ode45s solver was chosen to handle with the high nonlinearity of some parts. Also damping was added in a similar manner to simulate the coefficient of restitution of the endstop.

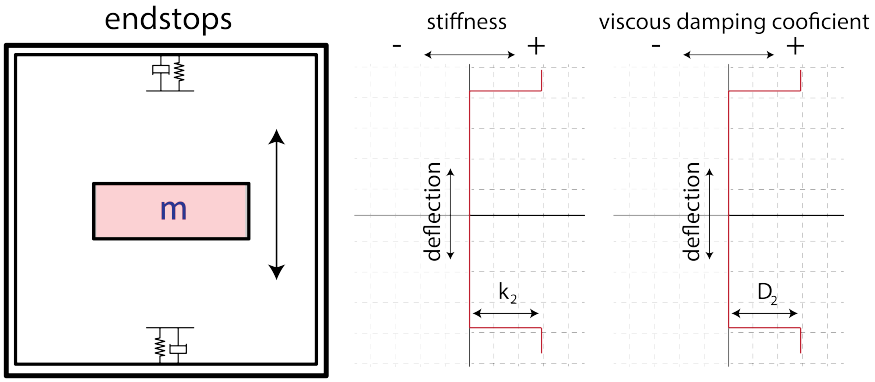

Figure 6.11: **mass endstops**

DAW ratchet force

To make this system An automatic winding device a ratchet has to be added. This was one of the most difficult parts to add. As a ratchet engaging or disengaging depends on the position and direction of travel in the past. The force this ratchet imposes on the mass was again modeled by using a tanh() function which would move with the proof mass. The teeth of the ratchet determine whether or not it engages and where it engages. So it was made so the tanh could move to the position where the ratchet would engage. When it is engaged it has to move at least a tooth length to store the energy. If not, the ratchet will just move back to the position it left off from and give the energy back to the proof masss. The Numerical model was set up with the ode45s solver, as the tanh() functions gave great changes in some inputs over time. Which the 45s is very good at solving.

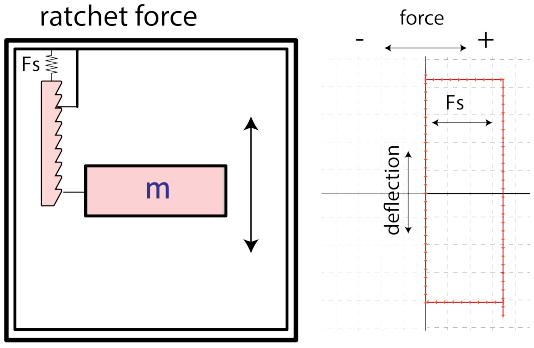

Figure 6.12: **DAW ratchet**

Tuning the Cooficient of restiution(COR) of the simuation was done by dropping the proof mass of the testsetup and looking at how it would bounce back when dropped from different heights. The spring stiffness of the suspension was determined by using releasing the mass and looking at the eigenfrequency as well as calculating the stiffness of a bended beam clamped at both ends. This gave similar results and thus was thought to be trustworthy. However later on the spring was removed as a whole, as the eigenfrequency of the whole suspension would be too high for good operation. Also in the end it would be better to have a zero or very low stiffness suspension for any reasonable power output. After the tuning the prototype came quite close to the simulation, however it was never exact.

The force of the ratchet with the DAW mechanism is shown is shown in Figure. **??**. This is the force when the mass moves up and down, as shown with the arrows in the graph. So the ratchet gives a force of 0 when it is moving backwards. Whilst it gives the force of the barrel spring when it moves forward. When the prove mass changes direction the force will stay the same for w while until the next tooth hooks on.

PDAW ratchet force

The force the DAW imposed on the mass was has always been constant. But with the PDAW installed it has a variable force acting on the mass. In fig.**??** the PDAW force acting on the mass is shown when looking at the angle of the mass. There is a certain range in the middle which is the point where the ratchet is not engaged due to the period doubling effect of the PDAW and the ratchet having a certain limit due to the distance between the teeth of the ratchet wheel.

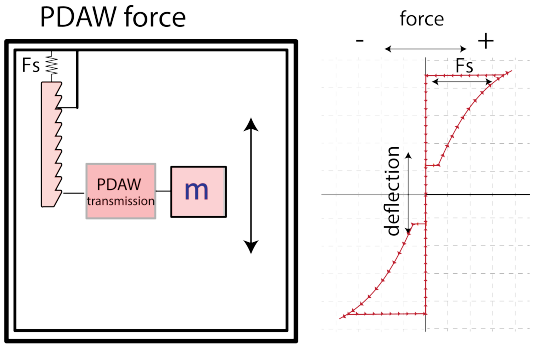

Figure 6.13: **DAW ratchet**

combining the components

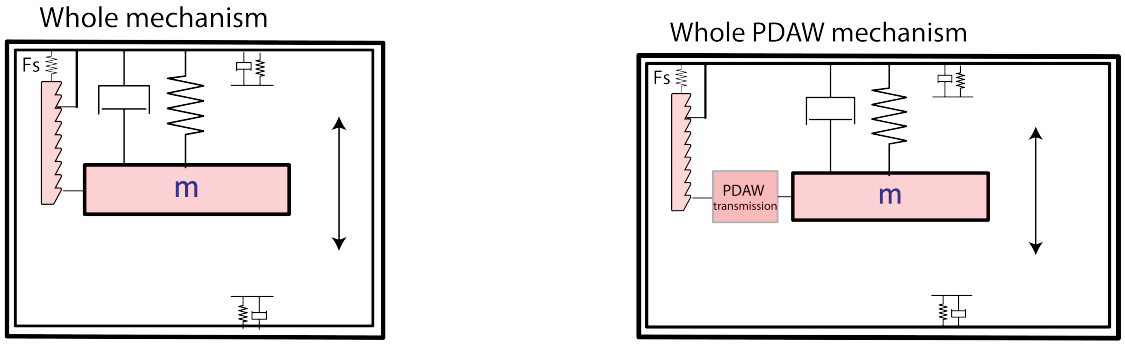

(a) DAW ratchet **(b)** DAW ratchet

Figure 6.14: **PDAW transmission prototype with motion**

The ratchet proved to be the mosty difficult to characterize as slight variations in assembly meant that the friction experienced by freewheeling would change. This would prove to be the biggest hurdle which I could not solve, and also I did not deem nessecary to solve to prove the mechanism. As improving the production method of the mechanism would get rid of these inconsistencies. also there where just a lot of variables which influenced the outcome of the measurements and the numerical model. Due to all the variables the effectiveness of the PDAW mechanism could not be excluded thus a different way was sought to proof the mechanism.

6.3 Quasi static analyses

6.3.1 concept

The third setup was radically different, to prove the mechanism I just needed the mechanism in it simplest form. Thus I decided to make it linear, with linear guides. The shaker was ditched as it could not provide the required displacements and frequencies. The goal is to show how it behaves in different acceleration fields. Thus a demonstrator was built and rotated in in and out of plane of gravity. This gave a way clearer view on how the mechanism performs under different accelerations. Also the numerical model was ditched and replaced by a quasi static model of the automatic winding device. This was combined with an analysis of the human walking gate and the corresponding wrist accelerations to estimate the energy output of the winding device. The quasi static model followed the prototype very well, except that the model did not include the friction of the linear guides and ball bearings. This gave a reduction in efficiency of about 20 % over the simulation.

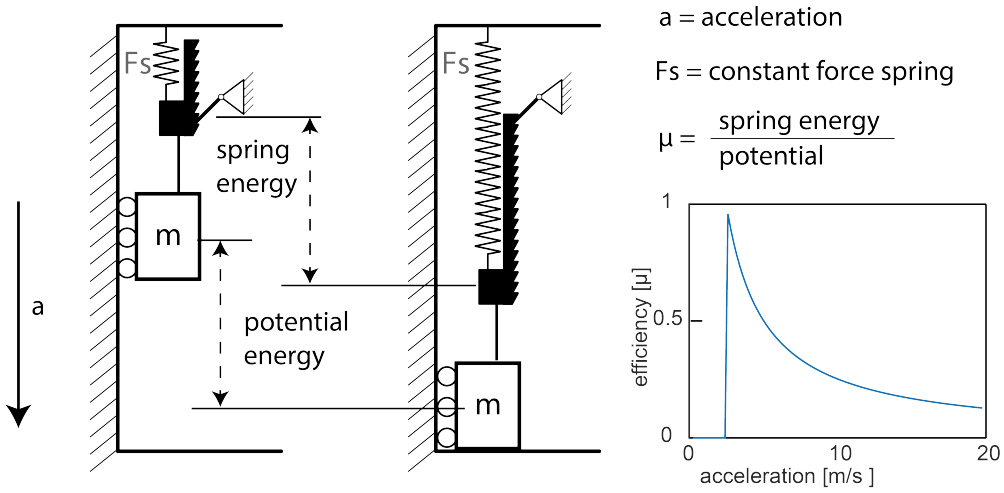

Figure 6.15: **quasi static eff calculation DAW**

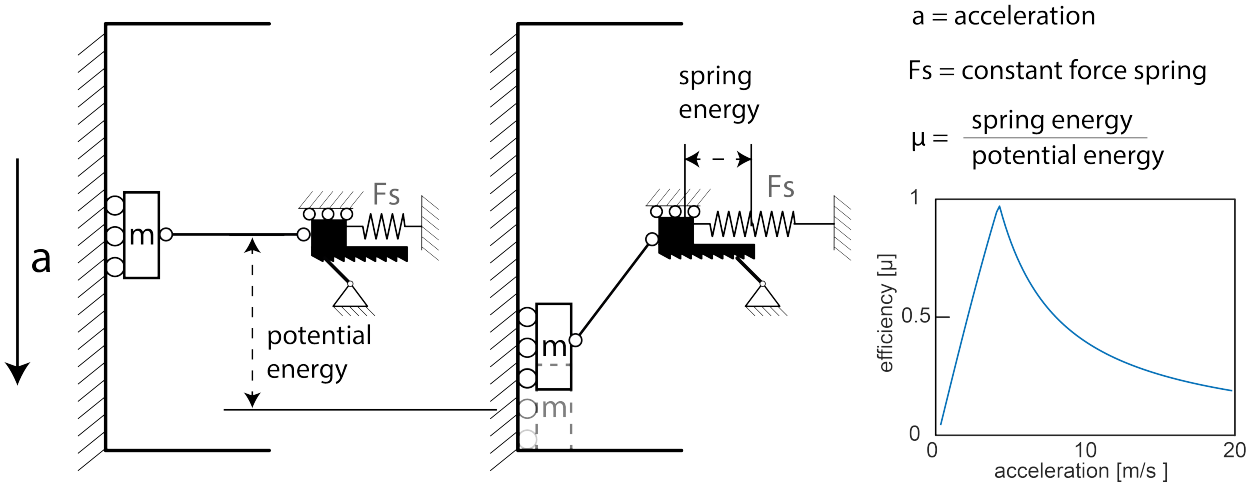

Figure 6.16: **quasi static eff calculation PDAW**

6.3.2 quasi static model

The quasi static model made of the PDAW is based on potential energy of the mass. If a mass has a certain height compared to an acceleration field it has a n energy potential. The energy potential of an automatic winding device is the length it can move internally. This is defined as the maximum energy which can be pulled from a certain acceleration. The accelerations are set as a constant. Then the mass is held in the middle of the motion range and released. With the quasi static model the point where the mass comes to rest is calculated. From this the energy stored in the barrel spring can be calculated for both the PDAW and the DAW. This stored energy can then be divided by the potential energy to give the efficiency of the mechanism under different accelerations.

The efficiency of these devices can be estimated by an analytical model. The starting situation is depicted in Figure 4(A) and Figure 4(B) with the inertial mass in the middle of its motion range. Then the mass is released under a constant acceleration. The spring with constant force F_s cannot return any energy to the system due to the ratchet. Thus the position where the proof mass will

come to rest will be the energy equilibrium of the spring and the mass. So first the energy stored in the spring must be determined, For the DAW this is:

$$(E_{s1}(D_{\text{in}}) = F_s D_{\text{in}} \tag{3}$$

Where E_{s1} is the energy stored in the spring, F_s is the force of the constant force spring and D_{in} is the displacement of the proof mass also shown in Figure 4(A). The energy stored in the PDAW is again dependent on the displacement of the spring.

$$(E_{s2} = F_s D_{\text{tr}} \tag{4}$$

Where E_{s2} is the energy stored in the PDAW spring, F_s is the force of the constant force spring D_{tr} is the extension of the constant force spring. D_{tr} is correlated with the proof mass displacement D_{in} via the Pythagoras theorem where:

$$(D_{\text{tr}} = L - \sqrt{L^2 - D_{\text{in}}2} \tag{5}$$

Where L is the length of the linkage. Substituting (2) and (3) gives the energy stored in the PDAW:

$$(E_{s2}(D_{\text{in}}) = Fs * (L - \sqrt{L^2 - D_{\text{in}}2}) \tag{6}$$

The potential energy due to the input acceleration is:

$$(E_a\,(D_{\text{in}}) = m a_{\text{in}} D_{\text{in}} \tag{7}$$

Where E_a is the potential energy, m the mass, a_{in} the input acceleration and d_{in} the proof mass displacement. If the mass moves is also dependent on the derivative of the potential energy, This will determine when the DAW will start to move and when not.

$$dEs<dEa \quad \textit{mass will move} \tag{8}$$

$$dEs>dEa \quad \textit{mass will not move} \tag{9}$$

$$(E_a(Din) = E_{s1,s2}(Din) \tag{10}$$

To compare both systems two design parameters are taken into consideration, $\alpha = F_s/F_a$ which is the spring force f_s divided by the inertial force of the mass f_a. This is a dimensionless value which can be used to determine the efficiency of the mechanism per acceleration, independently of scale and mass.

The second parameter is $\beta = d/l$ this defines the nonlinearity of the PDAW. This is the displacement range of the proof d mass over the length of the transmission rod L. This value has a maximum of 1 as the range of motion of the proof mas cannot exceed the length of the connecting rod. It is assumed when the mass hits the end stop all remaining kinetic energy will be dissipated. This is done to show the influence of the PDAW not the influence of the coefficient of restitution of the mass. The efficiency of the winding device can be calculated by dividing the energy stored in the spring by the maximum available work of the stroke.

$$\mu = \frac{\mathrm{E_{spring}}}{E_a(d)} \tag{11}$$

If we then substitute (2),(6),(9) and (10) we get for the DAW:

$$\mu_{s1} = \begin{cases} \alpha, & 0 < \alpha < 1 \\ 0, & a > 1 \end{cases} \tag{12}$$

The bound is where the acceleration becomes lower than the spring stiffness, here the mass will not move. Thus not storing any energy. If the acceleration just slightly higher the proof mass will hit the end stop, thus dissipating energy. The efficiency is shown in Figure 6(A) in the next section.

If we substitute (5), (6), (9) and (10) the efficiency of the PDAW is:

$$\mu_{s2} = \begin{cases} \frac{2}{\beta\alpha + \frac{\beta}{\alpha}}, & \beta < \frac{2}{\alpha + \frac{1}{\alpha}} \\ \frac{\alpha}{\beta}(1 - \sqrt{1 - \beta^2}), & \beta > \frac{2}{\alpha + \frac{1}{\alpha}} \end{cases} \tag{13}$$

The bounds again are where the proof mass hits the end stop of the AW device. But in the PDAW this is dependent on both the α and β. The efficiency of this mechanism is plotted in Figure 6(B) in the next section.

6.3.3 analysis human walking motion

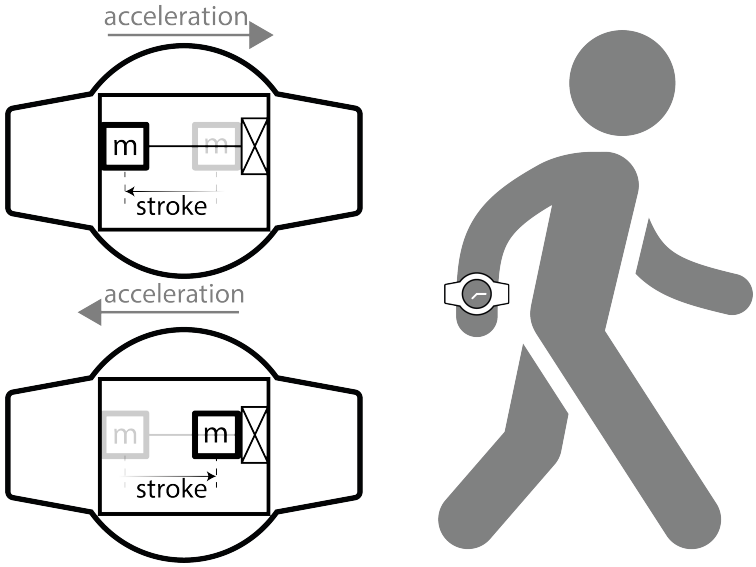

Figure 6.17: **automatic winding schematic with acceleration**

To estimate how an AW mechanism would behave on the human wrist, some analysis must be done on the wrist motion and on the underlying physics of such a mechanism. The winding mechanism in Figure 1 shows a proof mass that is able to move linearly, and it is rigidly connected to a mechanism that extracts energy. This mechanism houses the mainspring and the ratchet which allows it to also store this energy. No stiffness is added to the proof mass and the housing as this paper focuses on

improving the transmission mechanism from mass to mainspring. The limited stroke AW device shown in Figure 1 can generate power if the acceleration changes direction, and the mass is able to overcome the force imposed by the extraction mechanism and make a stroke. The intensity of these accelerations combined with the weight and displacement range of the proof mass will determine the maximum available energy per stroke with the formula:

$$E = mda \tag{14}$$

Where E is energy, m mass, d stroke length and a the average acceleration of a peak. Which is approximated with the peak acceleration and interpreting it as a sine curve. Thus a will be:

$$a = 2/pia_{peak} \tag{15}$$

The weight and internal displacement of an average proof mass in a watch are m=20g and d=10mm respectively. For the accelerations the database from [10] is used which contains acceleration data of the human wrist of 8 different subjects doing different activities. This database yields similar results as studies done for the human walking gate like [11], [12]. The displacement axis is chosen 18° so gravity has not to be accounted for. This angle is chosen as the average acceleration at this angle is 0, as most people do not point their wrist straight at the ground when they are walking. Shown in fig. 6.18. This is not the axis which houses the most power but it is done for simplifying the explanation.

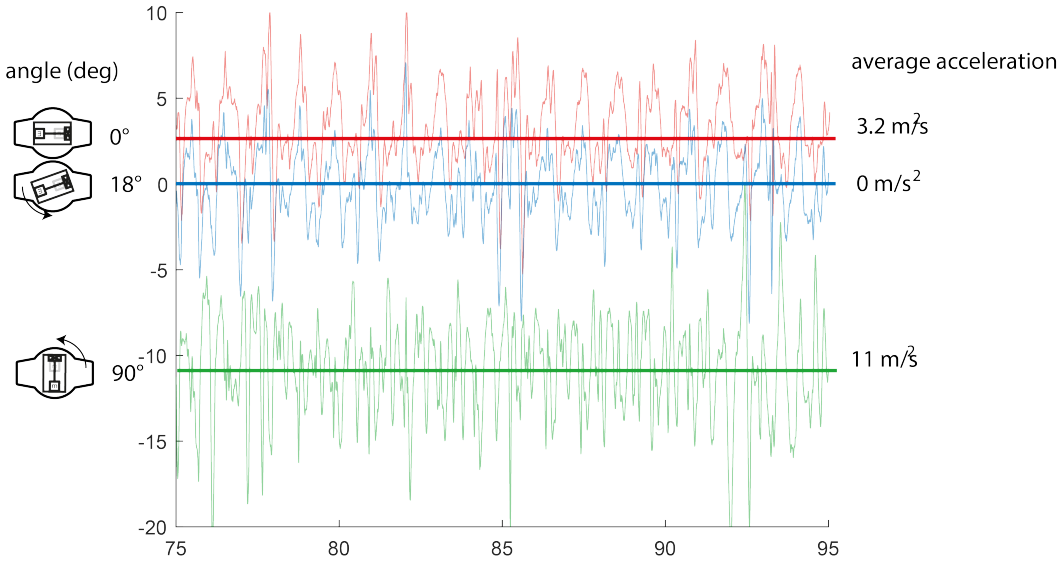

Figure 6.18: **the average accelerations on different axis acting on the winding device.**

This axis is analyzed by counting the acceleration peaks between 2 zero crossings shown in Figure 2 and adding them to a histogram. The peaks will be integrated twice over time to determine their displacement so false peaks with displacements smaller than 50% of the proof mass displacement can be discarded. These probably won't produce any power due to the accelerations being too low or short for the mass to overcome friction or they do not have any meaningful displacement. The residual counts are then evaluated with the formula (1) and (2) described earlier

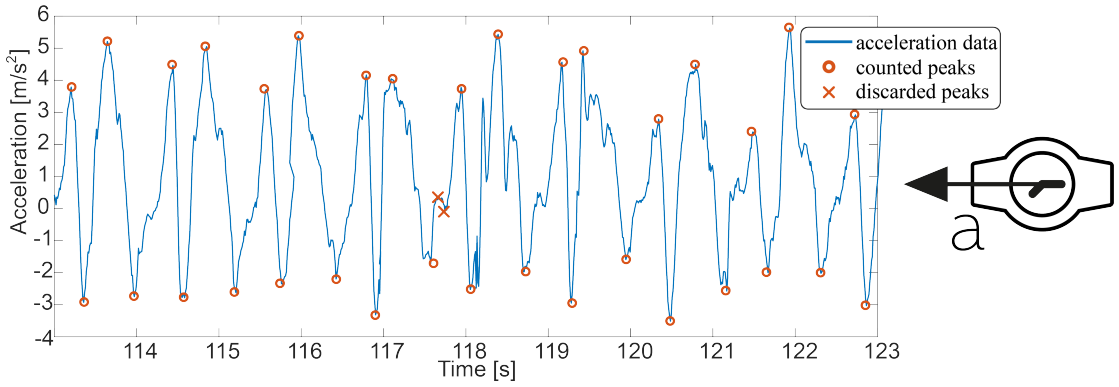

Figure 6.19: **acceleration peaks when walking. With counted and discarded peaks**

and normalized for time which will give an average power per acceleration. This is shown later in the results. With the average power per acceleration determined, the total power can be estimated if the efficiency of the transmission mechanisms is known at different accelerations.

Using the power histogram from human motion Figure 5(A), combined with (11) and (12) gives a power output for the mechanisms. With the mass 20g and displacment 10mm with the, F_v can be optimized by a line search for optimal power. F_s will determine the efficiency of the mechanisms over the acceleration range which can then be used to calculate the power output histogram of both the DAW and PDAW which are shown in Figure 5(B) and Figure 5(C) respectively. Taking the sum of this histogram gives an avarage power of both devices which is .56 mW for the DAW and .86mW for the PDAW. This is an 52% increase for the PDAW. This isncrease is mostly due to the fact that the PDAW can handle bot high and low accelerations, with the DAW the cutoff amplitude is clearly visible as for lower accelerations the power output is zero. in figure 6.20 the histogram from the 8 subjects is shown to create an average of them. However on an individual level that tended to differ quite a bit already as the some people move their hands much less whenever they are walking. this is clearly visible in the

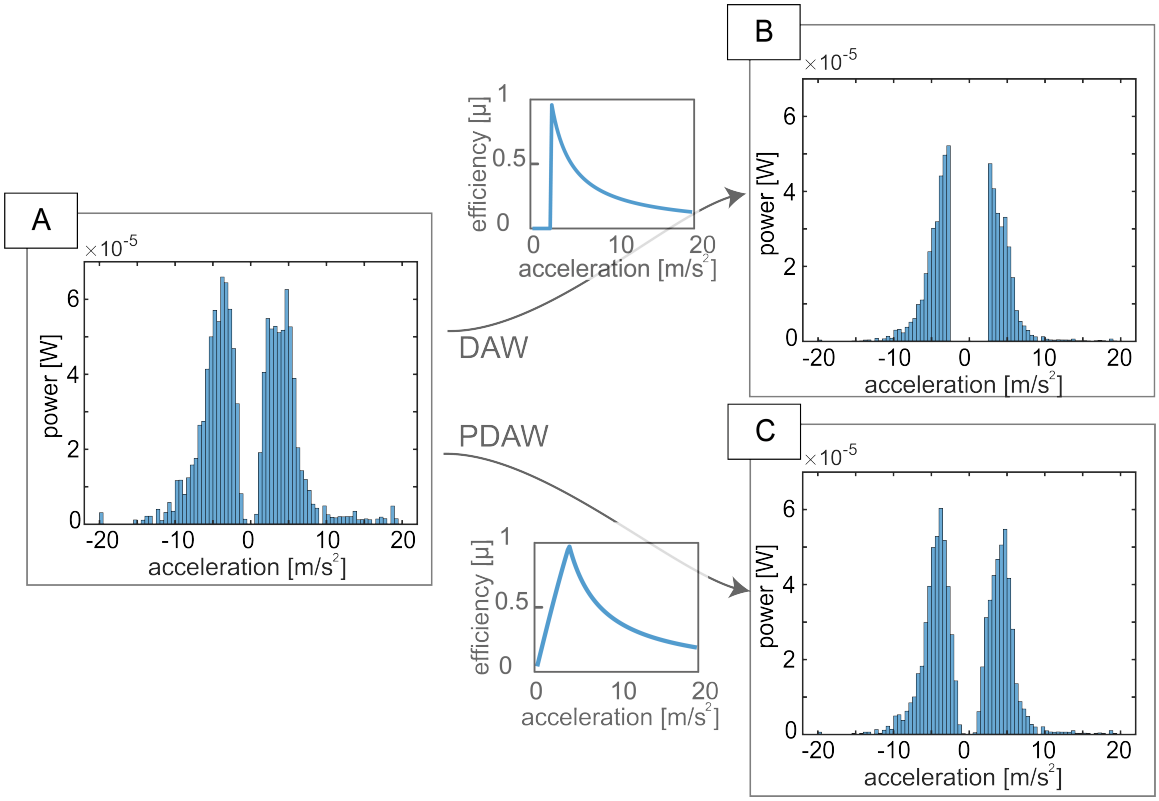

Figure 6.20: **(A)Power histogram for human walking motion. (B) power histogram for the DAW after the efficiency is taken into account (C) Power histogram for the PDAW after the efficiency is taken into account.**

6.3.4 quasi static prototype

Then the prototype was made to verify if the mechanism would actually follow the predicted curves of the efficiency. The prototype is shown in fig. **??** this was made with linear guides to be angled at different inclinations. So the gravity field acting on the mass changes in intensity. This will allow us to see how efficient the mechanism is at these intensities.

FOTO

all results are shown in appendix 2. it is clear that the mechanism behaves as expected. Te efficiency is 20% lower. This is to be expected as the simulation is not taking the friction of the guides and ball bearings into account. This was deemed not necessary, as this is highly dependent on the specific design.

6.3.5 choosing spring parameters

The force of the constant spring was chosen according to the analysis of the human motion. A linear line search was done on that force to see which would give the maximum power output of them mechanism. The power of the PDAW would always be larger then the DAW.

One of the most important parameters which I do not cover is the stiffness of the suspension mechanism inside the watch. The suspension should be a zero stiffness mechanism so the mass will move easily at every input motion. As the eigenfrequency of the proof mass must be below the input frequency. When designing a limited stroke winding mechanism this should definitely be included

as both the spring stiffness and orientation of the device are connected and pivotal to the energy output of the device. In the case of this research the mechanism was oriented in the vertical orientation. So gravity would not have to be compensated and just a zero stiffness suspension would do. If the mechanism would be orientated in more vertical. The stiffness of the suspension should compensate for that with some type of gravity balancing. This is better shown in figure6.18. One can imagine if the mechanism is designed at 18° it should have a stiffness of zero, or at least a stiffness low enough to create a low enough eigenfrequency. However if the 90° mechanism would have zero stiffness it would just lay flat on one of it's endstops, as it would not overcome the acceleration due to gravity. Thus not producing any power. If the mechanism would be made in this orientation one should not look to zero stiffness but to gravity compensation. Where the mass is suspended by a mechanism that creates a positive force equal to gravity, but no or very low stiffness. This will essentially 'compensate' for the acceleration due to gravity. Making this mechanism will be quite a difficult task, however not impossible. This solution will however not overcome the main drawbacks of limited stroke automatic winding which is the fact that if a winding device works well in a certain direction. One the person wearing it changes the orientation of the wrist, it stops working due to this 'gravity effect'. One can imagine that creating a mechanism for walking, wont work anymore if one starts wearing the watch upside down. On their left hand, or sits in a wheelchair. If limited stroke automatic winding will ever be implemented will depend on the decisions made for which tasks are chosen. Or some type of compensation mechanism should be conceived to compensate for rotating the wrist.

6.3.6 final design

Moving from the theoretical design to a physical design still has some hurdles. We can however give some insight. Designing the whole automatic winding mechanism will consist of four parts.
1.human motion analyses
2.suspension
3.ratchet
4.transmission
The required activities should be chosen, and from these activities the best orientation should be decided on. Here not only power should be taken into account, but also all possible users(people in wheelchairs, wearing the watch in a different way etc.). When the orientation is chosen the suspension can be designed to create a zero stiffness compensated suspension. then the ratchet should be fit in to be made as small as possible with as many teeth as possible. after that the PDAW should be designed in combination with the force of the constant force spring. Then the mechanism should look as shown in fig6.21. In this example the a buckling beam is used with negative stiffness to oppose the suspension stiffness. This could be any stiffness compensation mechanism.

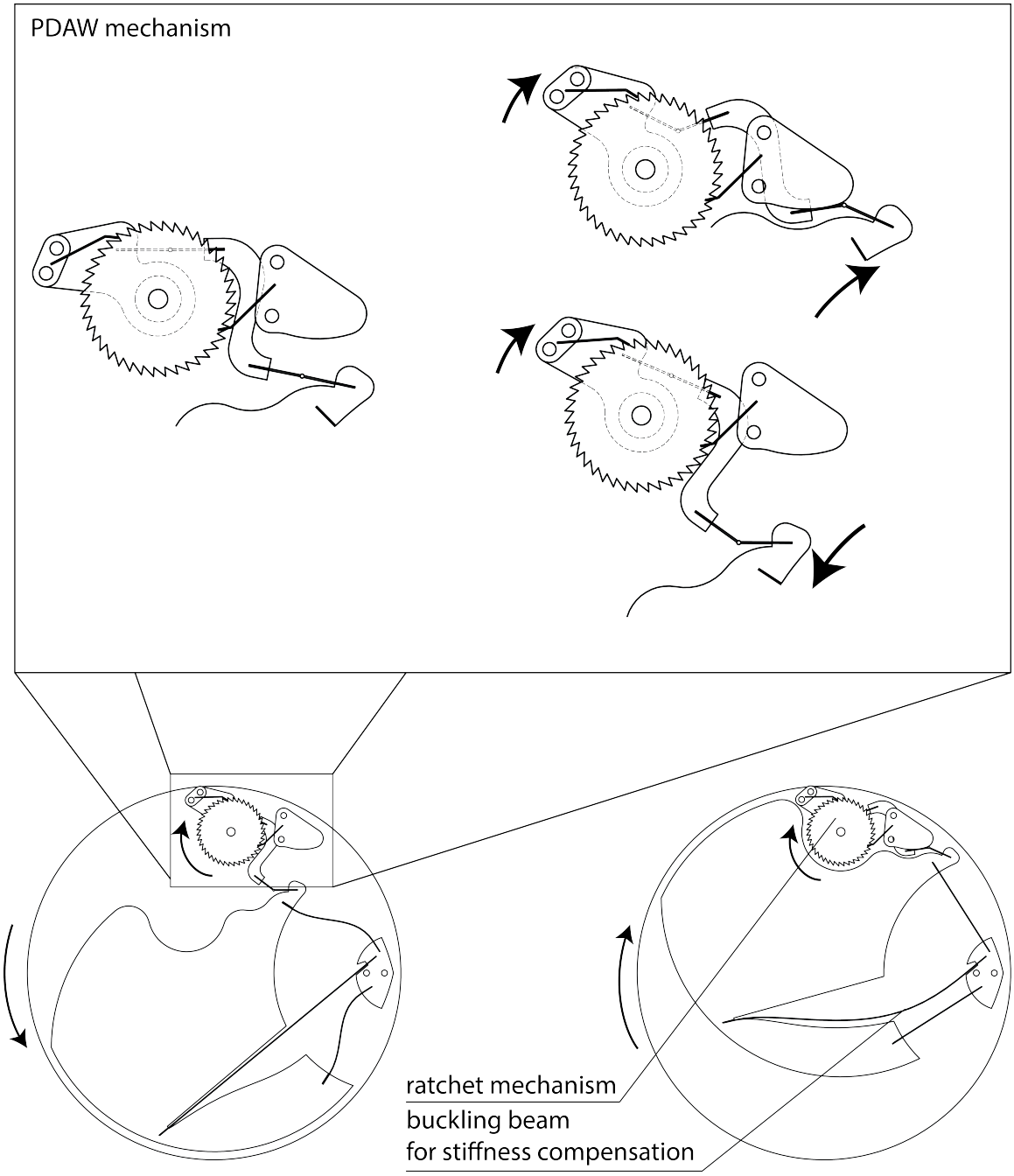

Figure 6.21: **example of what the full PDAW mechanism could look like in a watch.**

6.4 numerical model DAW results

The next graphs show the PDAW winding at different accelerations.

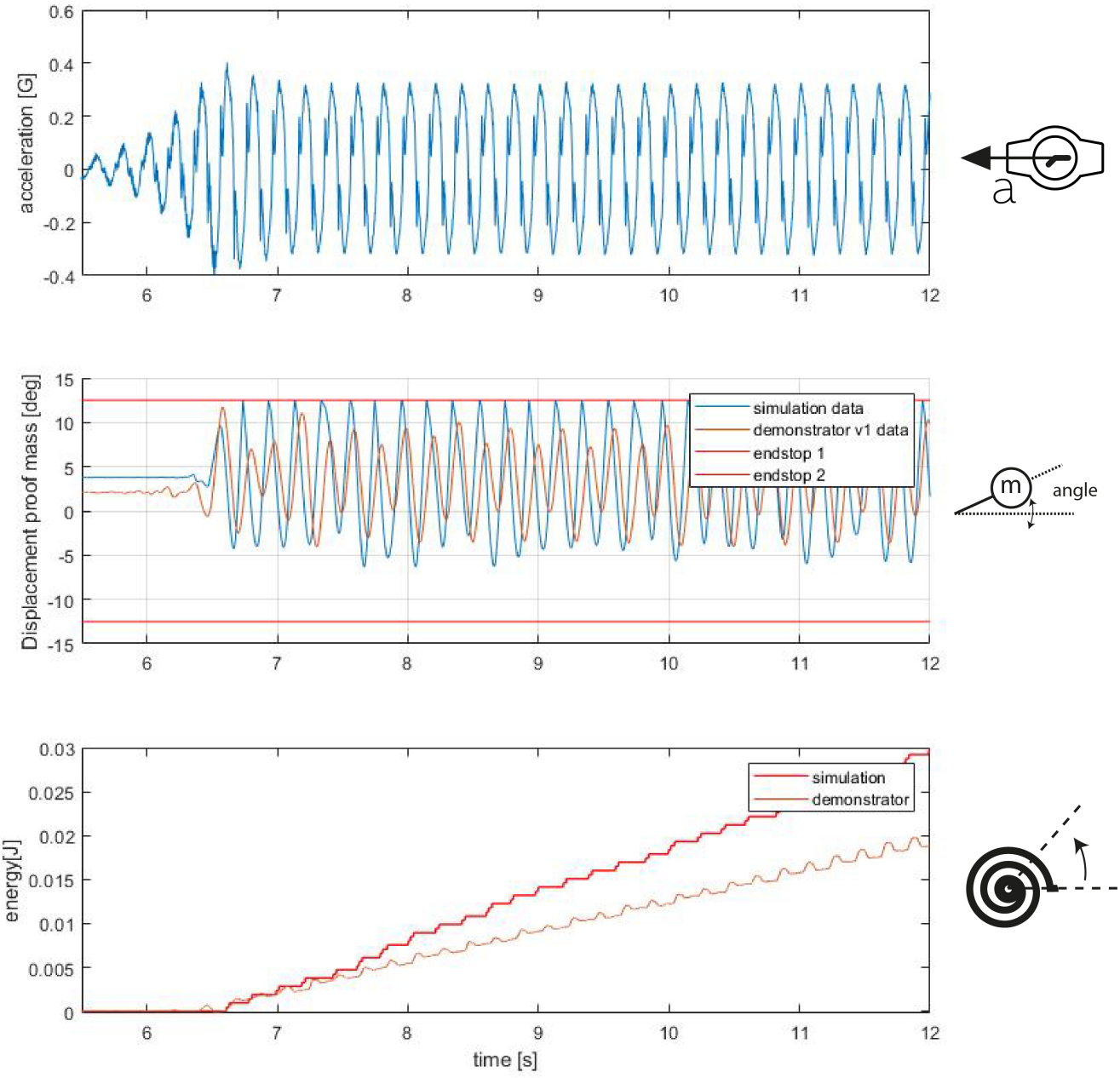

Figure 6.22: **numerical simulation of the DAW compared to demonstrator with input amplitude of .3G at 5Hz**

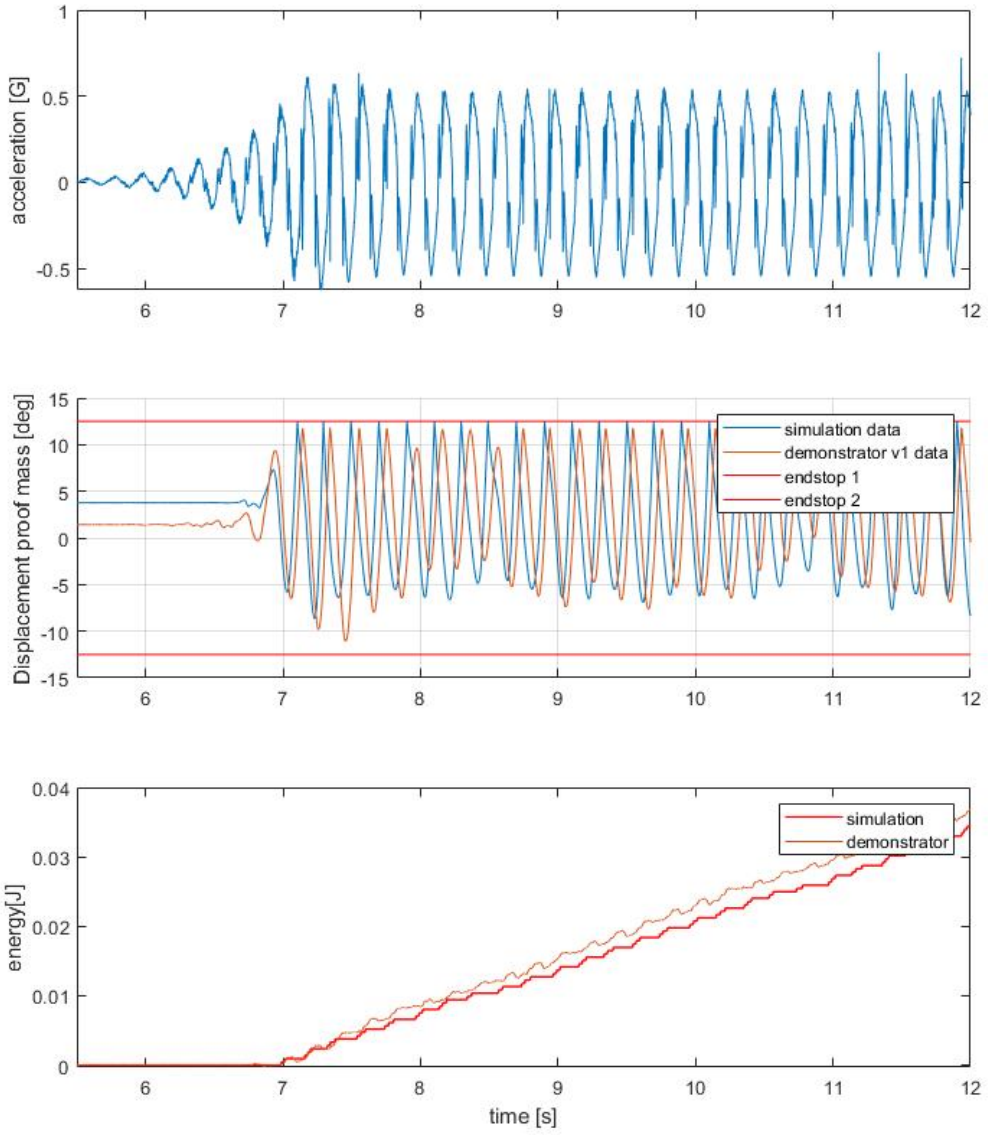

Figure 6.23: **numerical simulation of the DAW compared to demonstrator with input amplitude of .5G at 5Hz**

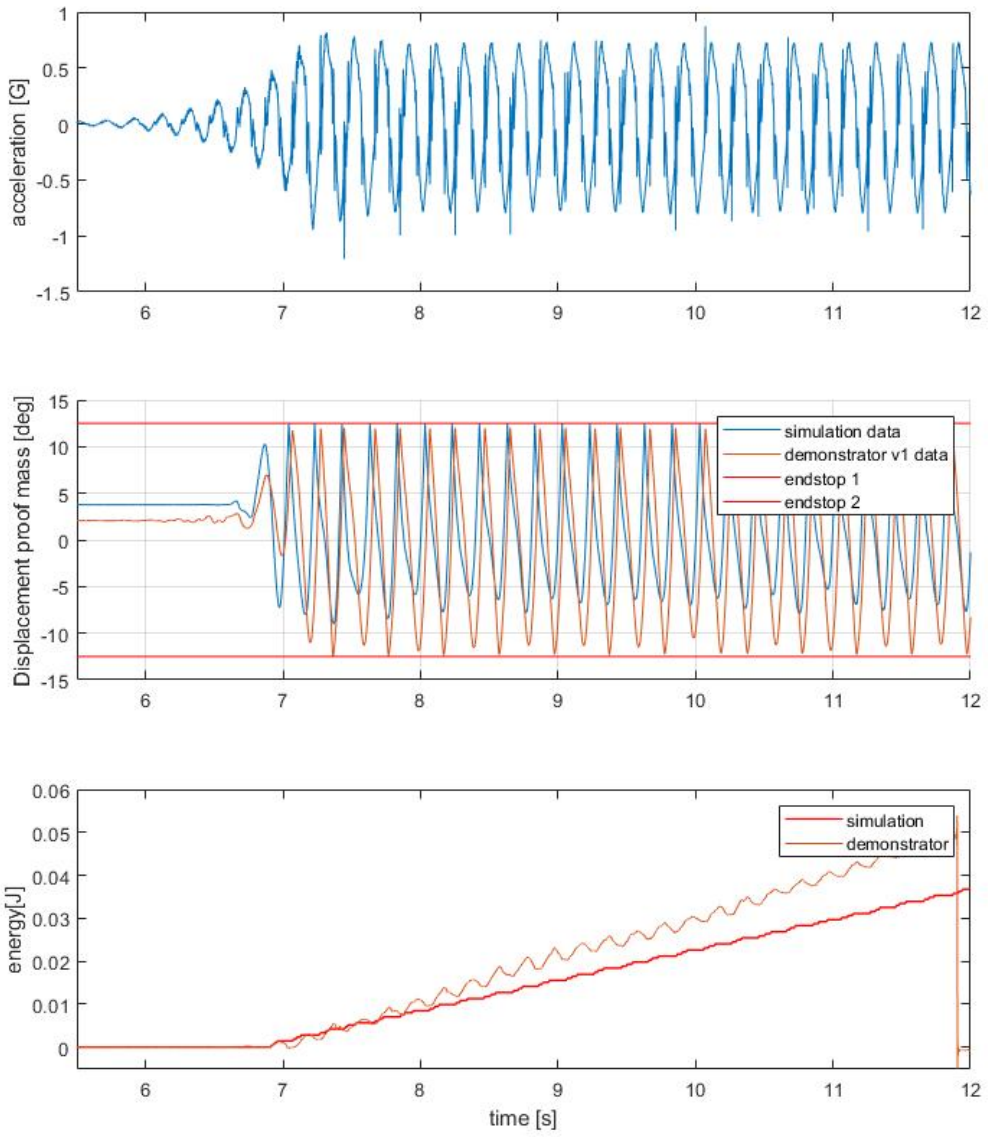

Figure 6.24: **numerical simulation of the DAW compared to demonstrator with input amplitude of .7G at 5Hz**

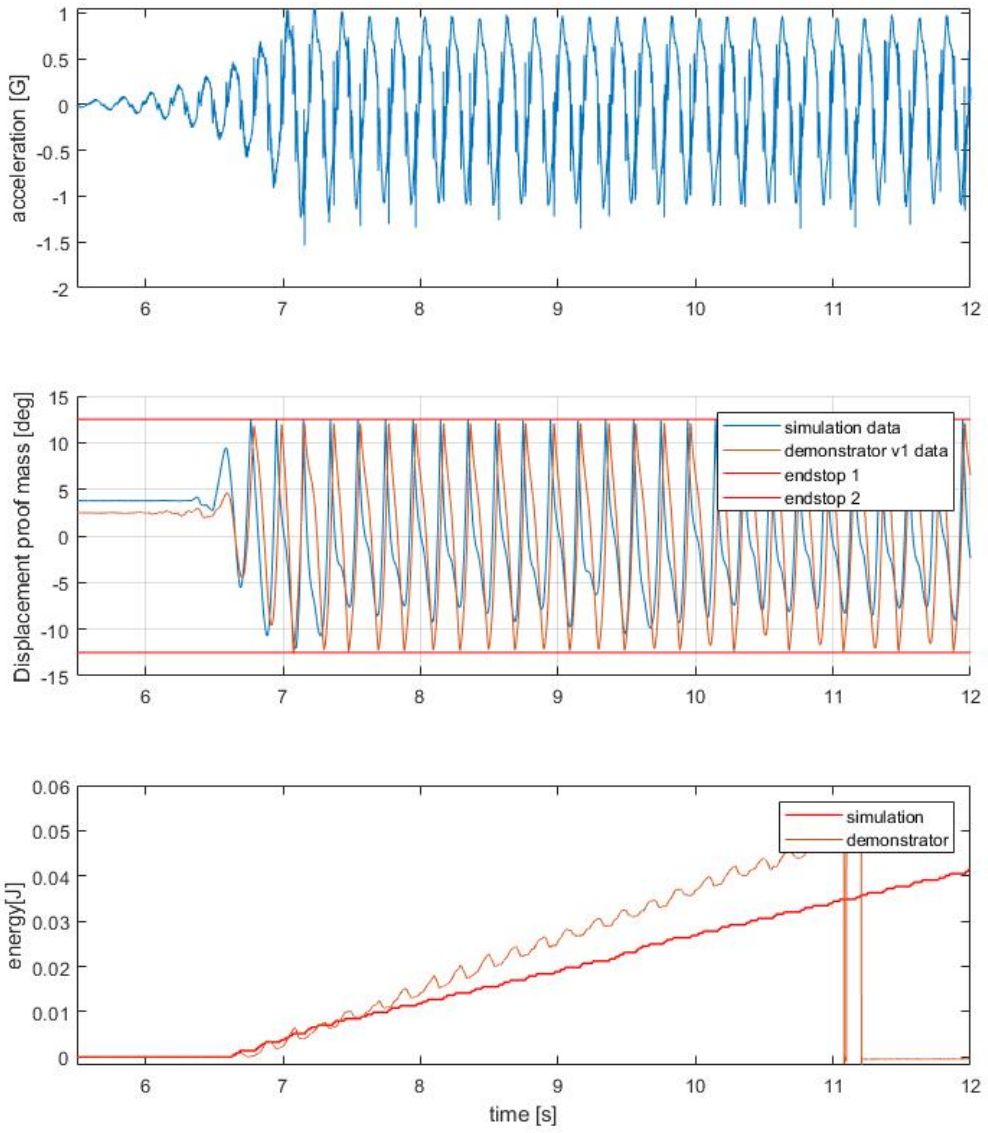

Figure 6.25: **numerical simulation of the DAW compared to demonstrator with input amplitude of .9G at 5Hz**

6.5 numerical model PDAW

The next graphs show the PDAW winding at different accelerations.

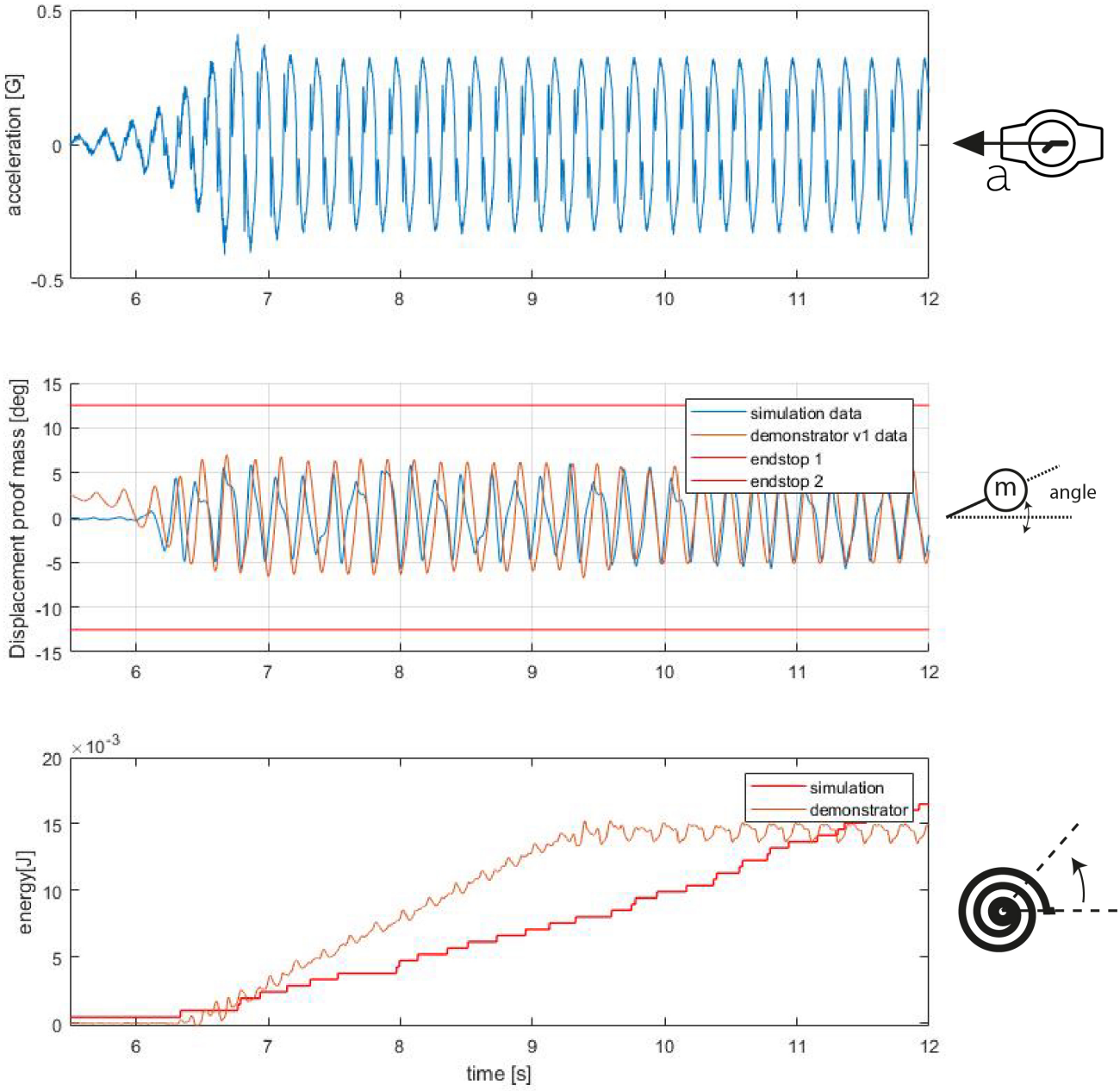

Figure 6.26: **numerical simulation of the PDAW compared to demonstrator with input amplitude of .3G at 5Hz**

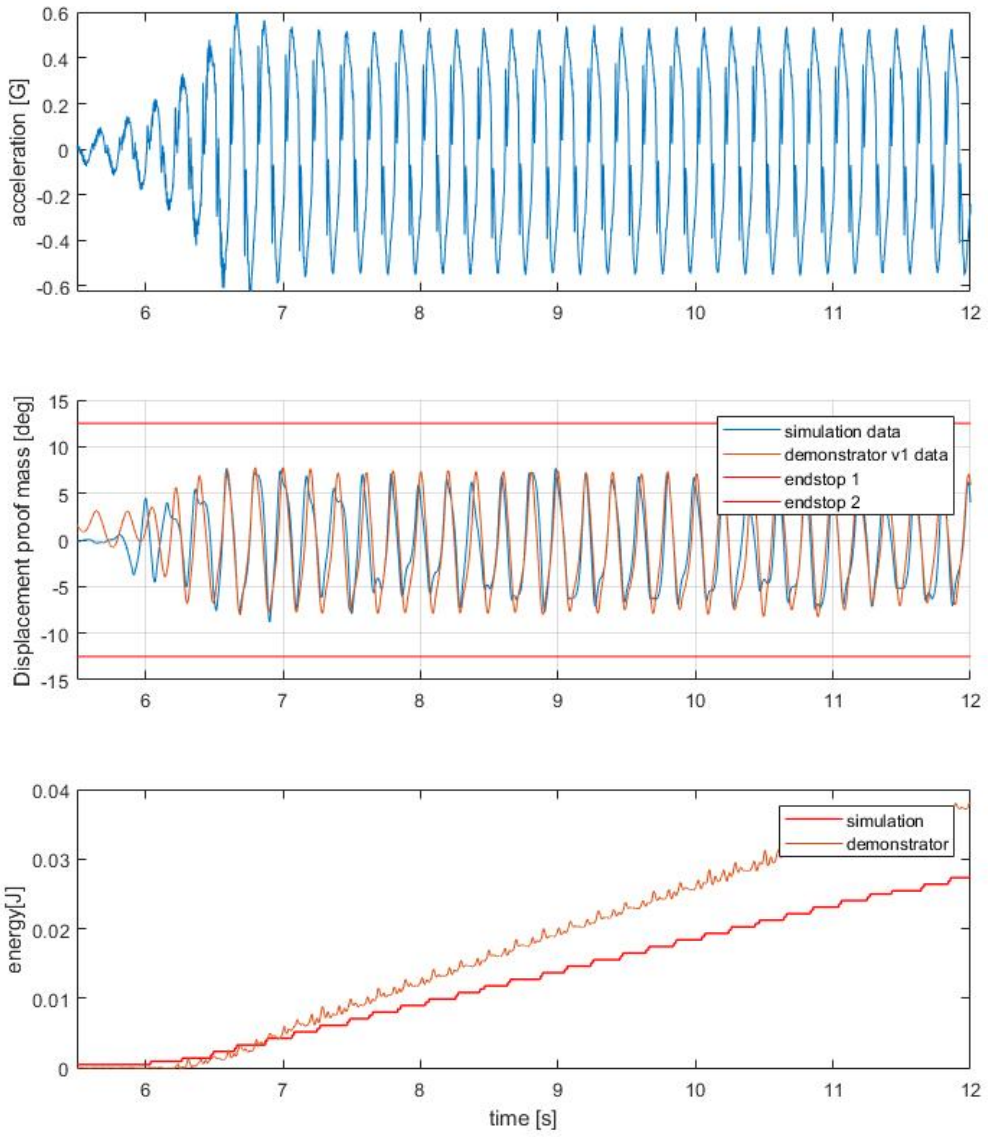

Figure 6.27: **numerical simulation of the PDAW compared to demonstrator with input amplitude of .5G at 5Hz**

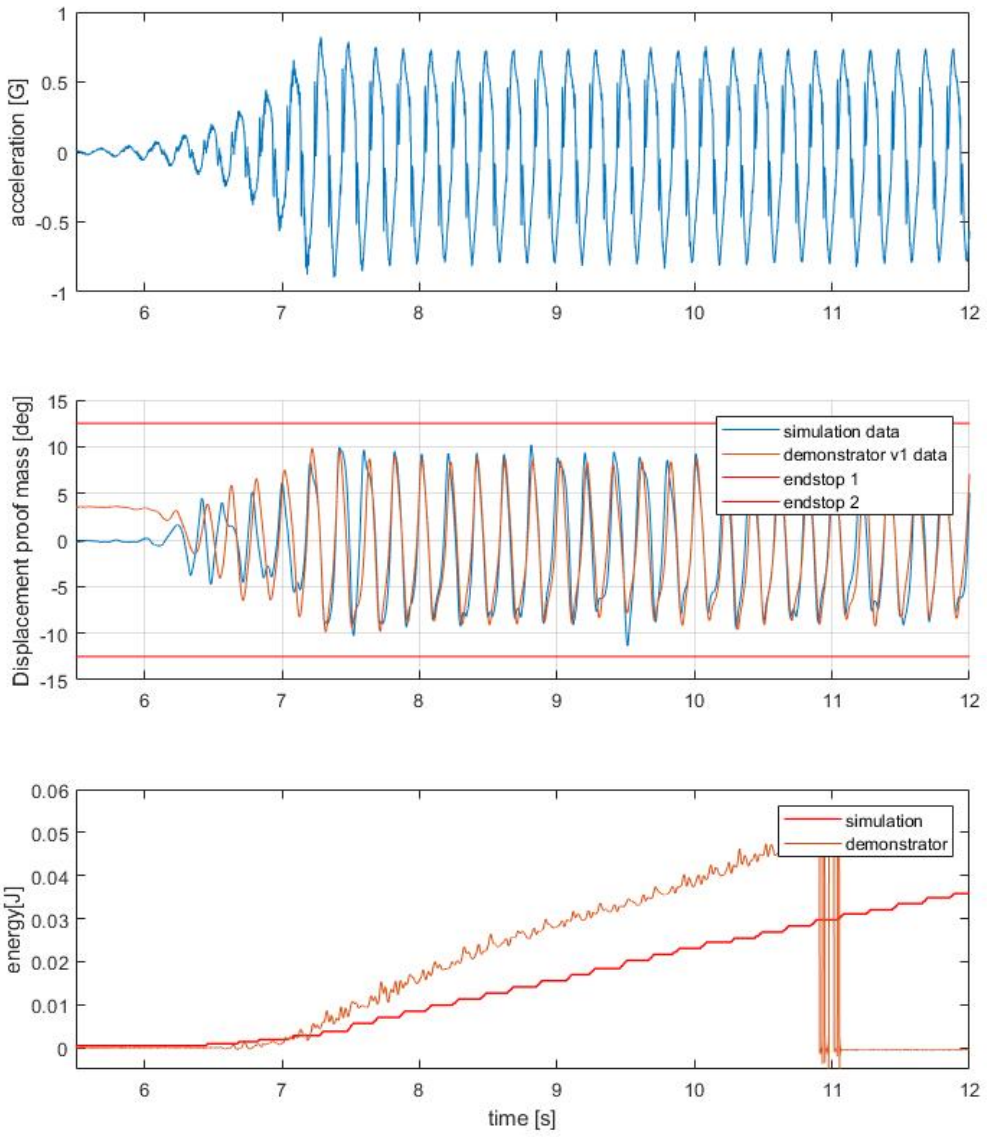

Figure 6.28: **numerical simulation of the PDAW compared to demonstrator with input amplitude of .7G at 5Hz**

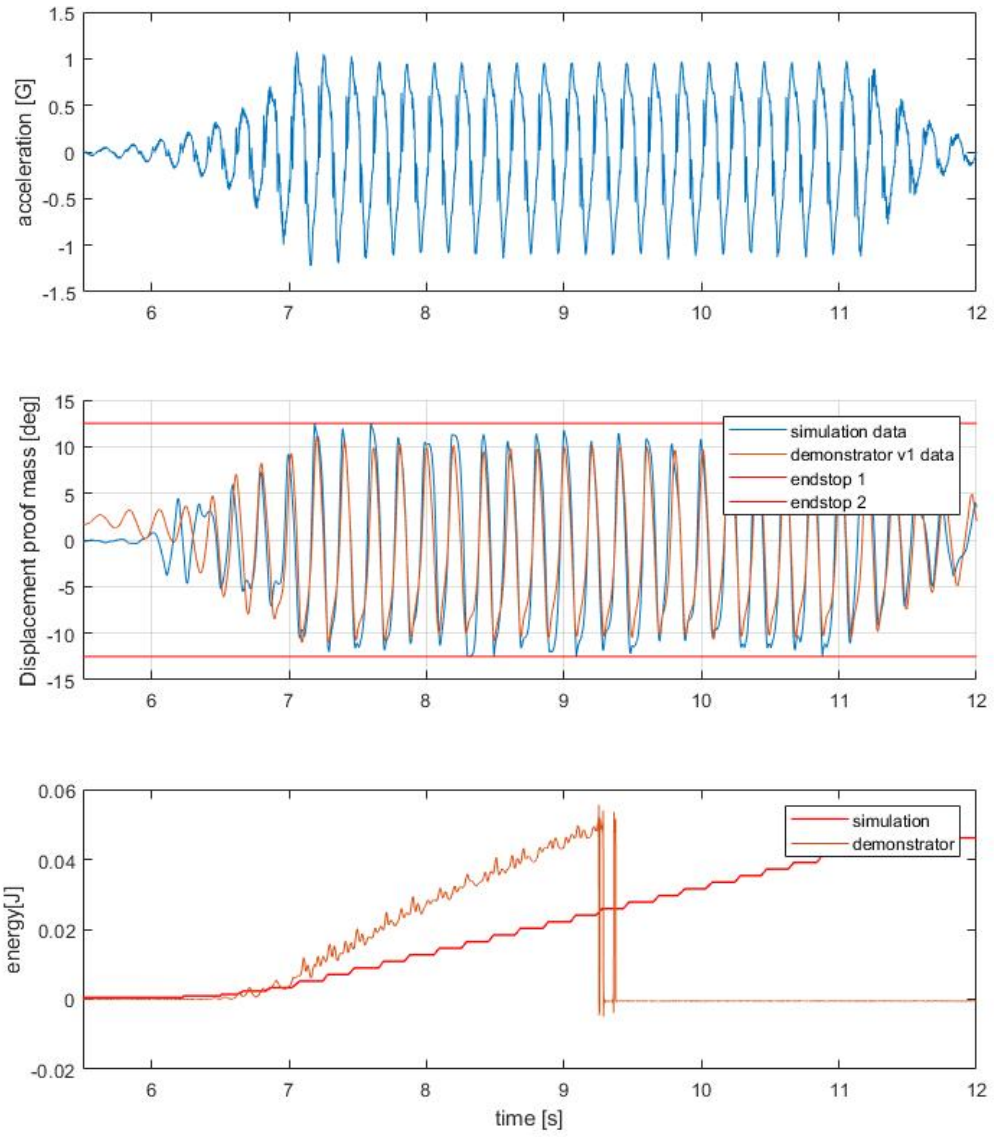

Figure 6.29: **numerical simulation of the PDAW compared to demonstrator with input amplitude of .9G at 5Hz**

6.6 DAW quasi-static performance

This shows the performance of the quasi static simulation compared to the measured values of the DAW prototype. The drop in efficiency due to friction is clearly visible.

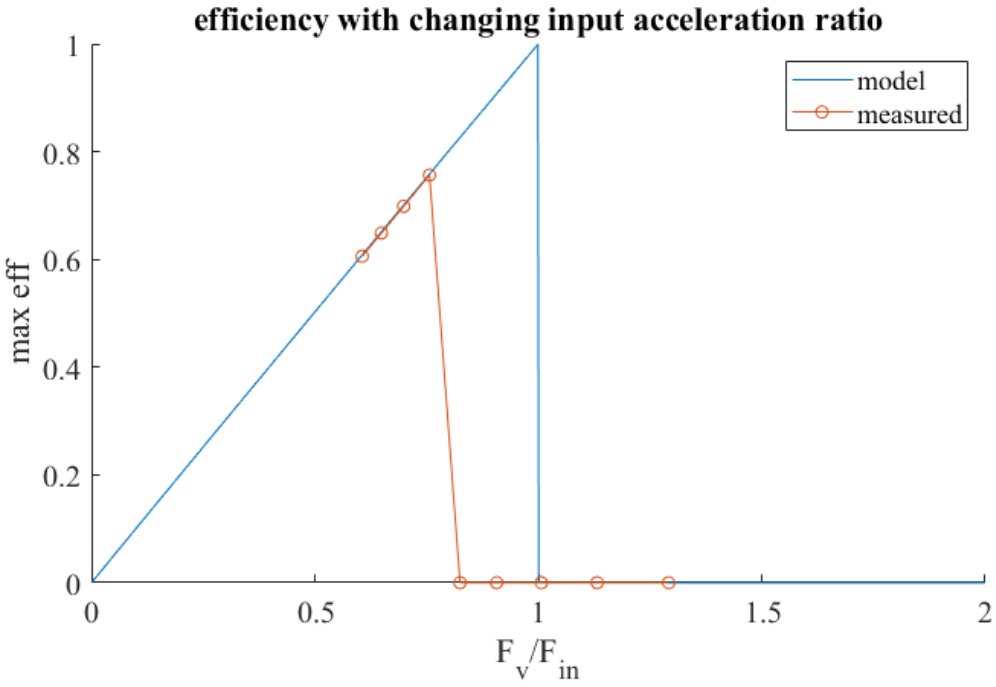

Figure 6.30: **DAW quasi static simulation and prototype**

6.7 PDAW quasi-static performance

This shows the performance of the quasi static simulation compared to the measured values of the PDAW prototype. The drop in efficiency due to friction is clearly visible.

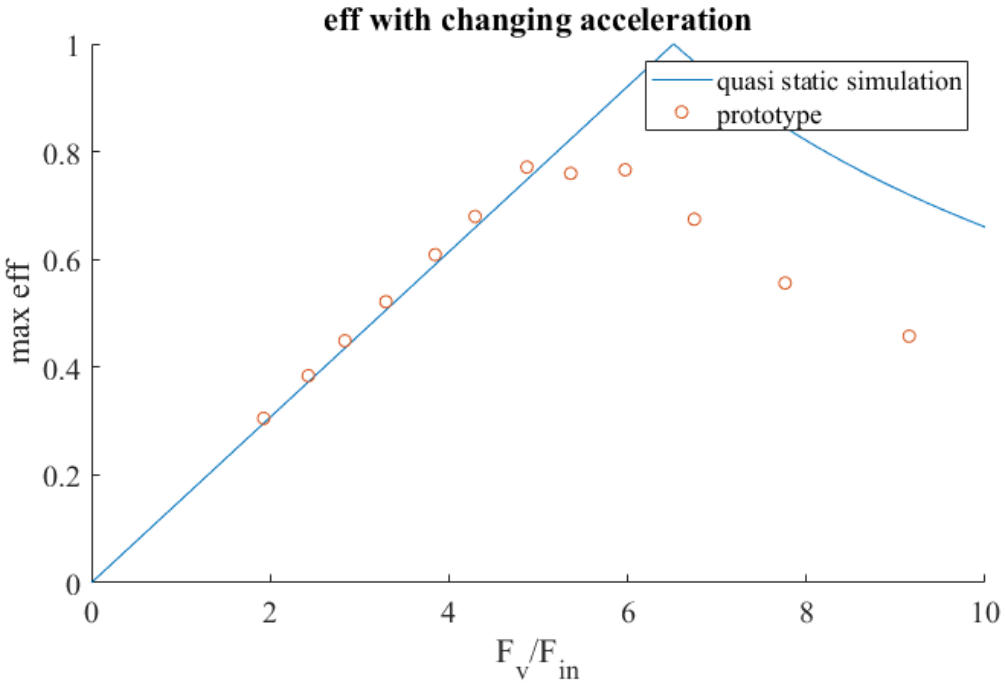

Figure 6.31: **PDAW quasi static simulation and prototype beta=0.3**

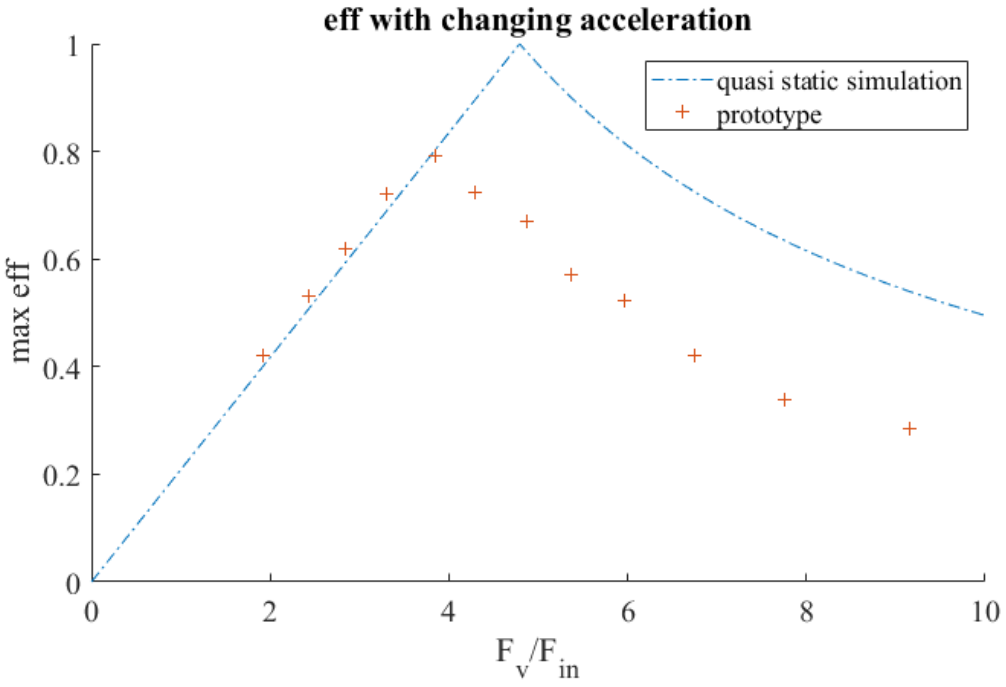

Figure 6.32: **PDAW quasi static simulation and prototype beta=0.4**

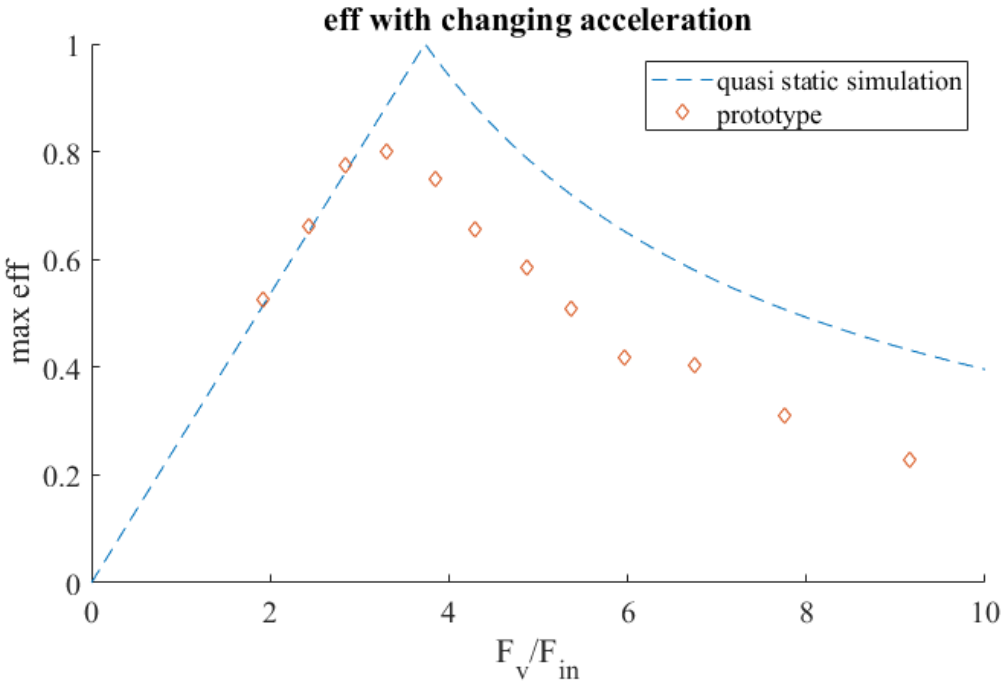

Figure 6.33: **PDAW quasi static simulation and prototype beta=0.5**

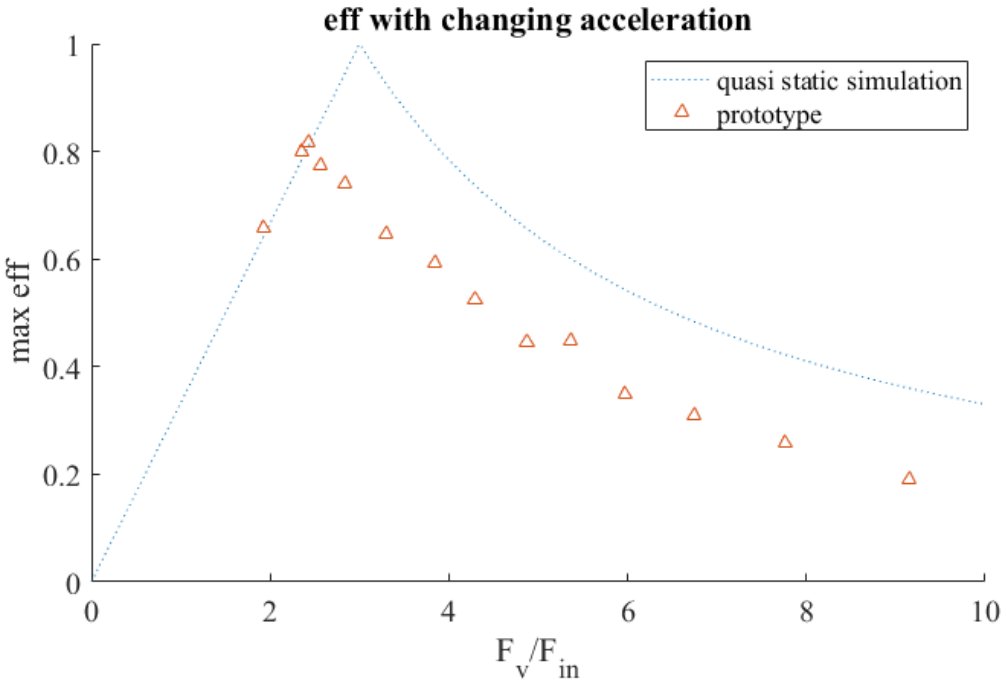

Figure 6.34: **PDAW quasi static simulation and prototype beta=0.6**

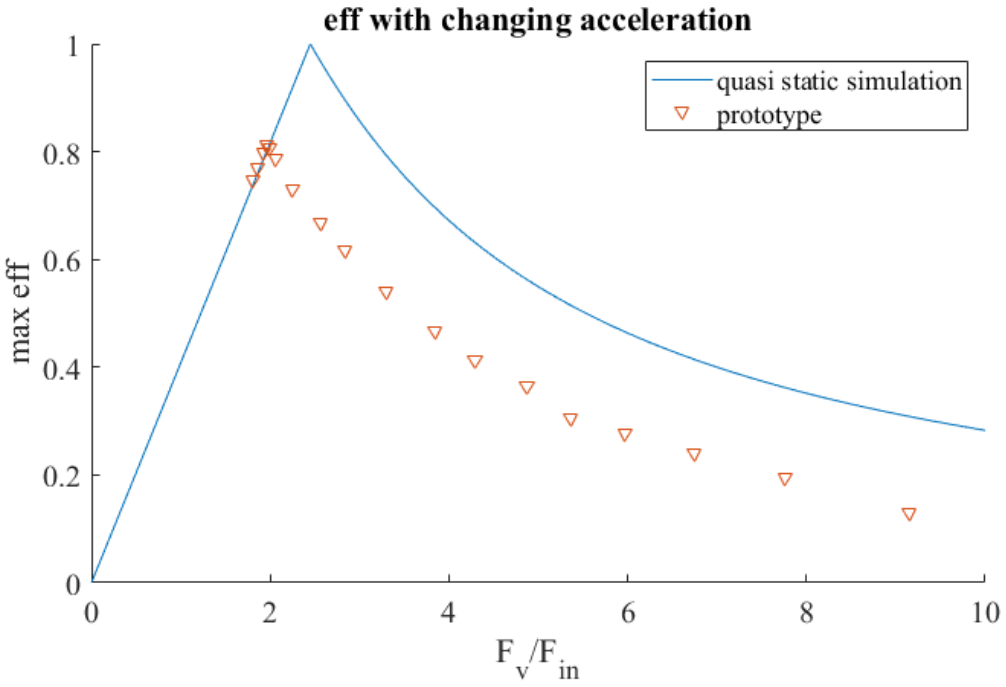

Figure 6.35: **PDAW quasi static simulation and prototype beta=0.7**

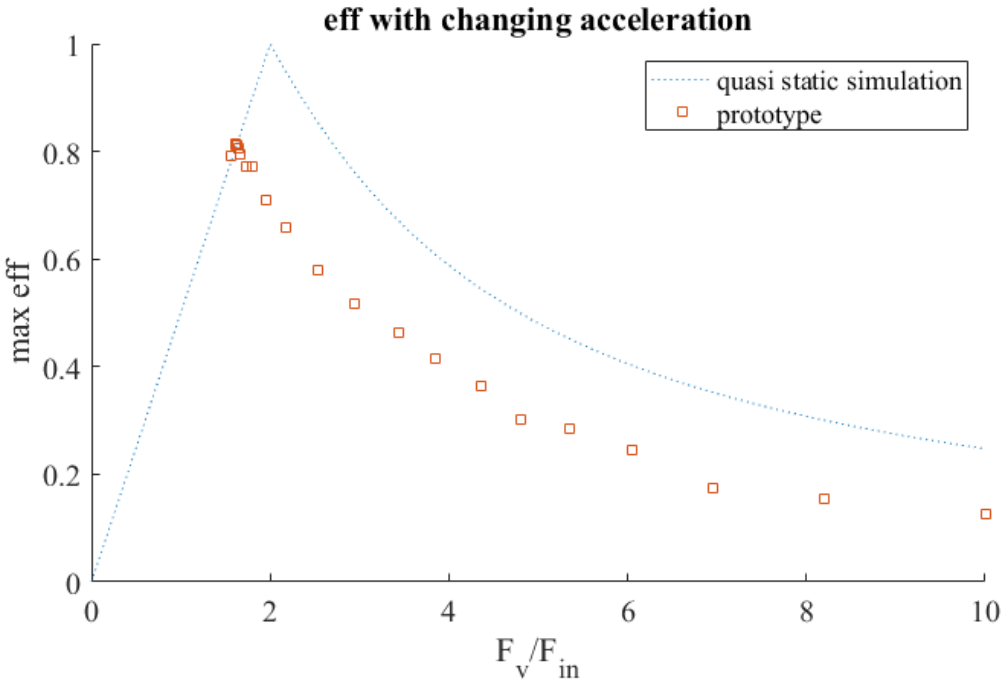

Figure 6.36: **PDAW quasi static simulation and prototype beta=0.8**

References

[1] P. D. Mitcheson, E. M. Yeatman, G. K. Rao, A. S. Holmes, and T. C. Green, "Energy harvesting from human and machine motion for wireless electronic devices," *Proceedings of the IEEE*, vol. 96, no. 9, pp. 1457–1486, 2008.

[2] J. Yun, S. Patel, M. Reynolds, and G. Abowd, "A quantitative investigation of inertial power harvesting for human-powered devices," *UbiComp 2008 - Proceedings of the 10th International Conference on Ubiquitous Computing*, pp. 74–83, 2008.

[3] Z. Yang, A. Erturk, and J. Zu, "On the efficiency of piezoelectric energy harvesters," *Extreme Mechanics Letters*, vol. 15, pp. 26–37, 2017. [Online]. Available: http://dx.doi.org/10.1016/j.eml.2017.05.002

[4] A. Reiss, "Personalized Mobile Physical Activity Monitoring for Everyday Life Attila Reiss," no. January, 2014.

[5] A. M. Eltanany, T. Yoshimura, N. Fujimura, M. R. Ebied, and M. G. S. Ali, "Development of piezoelectric bistable energy harvester based on buckled beam with axially constrained end condition for human motion."

[6] S. Materials, "A review of the recent research on vibration energy harvesting via bistable systems," 2013.

[7] P. Pillatsch, L. M. Miller, E. Halvorsen, P. K. Wright, E. M. Yeatman, and A. S. Holmes, "Self-tuning behavior of a clamped-clamped beam with sliding proof mass for broadband energy harvesting," *Journal of Physics: Conference Series*, vol. 476, no. 1, 2013.

[8] P. L. Green, E. Papatheou, and N. D. Sims, "Energy harvesting from human motion and bridge vibrations: An evaluation of current nonlinear energy harvesting solutions," *Journal of Intelligent Material Systems and Structures*, vol. 24, no. 12, pp. 1494–1505, 2013.

[9] C. Tudor-Locke, W. D. Johnson, and P. T. Katzmarzyk, "Accelerometer-determined steps per day inus adults," *Medicine and Science in Sports and Exercise*, vol. 41, no. 7, pp. 1384–1391, 2009.

[10] T. Harms, J. Gershuny, A. Doherty, E. Thomas, K. Milton, and C. Foster, "A validation study of the Eurostat harmonised European time use study (HETUS) diary using wearable technology," *BMC Public Health*, vol. 19, no. Suppl 2, pp. 55–59, 2019.

[11] A. H. Montoye, B. S. Westgate, M. R. Fonley, and K. A. Pfeiffer, "Cross-validation and out-of-sample testing of physical activity intensity predictions with a wrist-worn accelerometer," *Journal of Applied Physiology*, vol. 124, no. 5, pp. 1284–1293, 2018.

[12] P. D. Mitcheson, P. Miao, B. H. Stark, E. M. Yeatman, A. S. Holmes, and T. C. Green, "MEMS electrostatic micropower generator for low frequency operation," *Sensors and Actuators, A: Physical*, vol. 115, no. 2-3 SPEC. ISS., pp. 523–529, 2004.

[13] M. F. Daqaq, "Nonlinear Analysis of Axially," vol. 133, no. February 2011, 2013.

[14] S. Zhou, J. Cao, D. J. Inman, J. Lin, S. Liu, and Z. Wang, "Broadband tristable energy harvester: Modeling and experiment verification," *Applied Energy*, vol. 133, pp. 33–39, 2014. [Online]. Available: http://dx.doi.org/10.1016/j.apenergy.2014.07.077

[15] J. Cao, W. Wang, S. Zhou, D. J. Inman, and J. Lin, "Nonlinear time-varying potential bistable energy harvesting from human motion," *Applied Physics Letters*, vol. 107, no. 14, 2015. [Online]. Available: http://dx.doi.org/10.1063/1.4932947

[16] K. Wang, J. Zhou, H. Ouyang, Y. Chang, and D. Xu, "A dual quasi-zero-stiffness sliding-mode triboelectric nanogenerator for harvesting ultralow-low frequency vibration energy," *Mechanical Systems and Signal Processing*, vol. 151, p. 107368, 2021. [Online]. Available: https://doi.org/10.1016/j.ymssp.2020.107368

[17] P. D. Mitcheson, T. C. Green, E. M. Yeatman, and A. S. Holmes, "Architectures for vibration-driven micropower generators," *Journal of Microelectromechanical Systems*, vol. 13, no. 3, pp. 429–440, 2004.

[18] T. V. Büren, P. D. Mitcheson, T. C. Green, E. M. Yeatman, A. S. Holmes, and G. Tröster, "Optimization of Inertial Micropower Generators for Human Walking Motion," vol. 6, no. 1, pp. 28–38, 2006.

[19] A. H. Hosseinloo and K. Turitsyn, "Fundamental Limits to Nonlinear Energy Harvesting," vol. 064009, pp. 1–8, 2015.